Regional tilt of the Mount Stuart batholith, Washington, determined using aluminum-in-hornblende barometry: Implications for northward translation of Baja British Columbia

Jay J. Ague } *Department of Geology and Geophysics, Yale University, P.O. Box 208109,*
Mark T. Brandon } *New Haven, Connecticut 06520-8109*

ABSTRACT

We have developed a new quantitative method to estimate paleohorizontal in granitic plutons using the aluminum-in-hornblende (AH) barometer. The method is used to correct previously published paleomagnetic data from the 93–96 Ma Mount Stuart batholith of the Cascades Mountains, Washington State, for the effects of postemplacement tilting. AH barometry was done on 46 samples from the batholith using the compositions of hornblende rims coexisting with the full mineral assemblage required for pressure estimation. High-contrast back-scattered electron imaging was used to ensure that the analyzed hornblendes were not significantly affected by subsolidus alteration.

The success of the AH barometry is indicated by two observations. First, increases in the Al content of the hornblendes are governed almost entirely by a pressure-sensitive *tschermak*-type substitution. Second, amphibole-plagioclase thermometry indicates that assemblage equilibration occurred at or very near magmatic conditions ($\approx 650\,°C$) and that temperature has a negligible effect on our pressure estimates. AH barometry results indicate that the depth of crystallization across the batholith decreases systematically from ≈ 0.3 GPa in the northwest to ≈ 0.15 GPa in the southeast, consistent with independent barometry for the contact aureole of the batholith and regional structural and stratigraphic relations. Using a best-fit planar-tilt model and bootstrap analysis of uncertainties, we estimate that the paleohorizontal plane has a strike of $43° \pm 30.4°$ and dip of $7° \pm 2.0°$ southeast ($\pm 95\%$ confidence).

Our estimated paleohorizontal allows us to restore the paleomagnetic data of Beck et al. (1981) and to estimate the original paleolatitude of the Mount Stuart batholith. Beck et al. found that the southern part of the batholith yielded a number of sites with a well-defined high-coercivity remanence. The carrier of this remanence was not resolved, but the following four lines of evidence strongly suggest that the published directions were acquired shortly after emplacement of the batholith. (1) The "stable" sites all came from the shallowest and most rapidly cooled portions of the batholith as indicated by our AH results and concordant K/Ar ages for hornblende/biotite pairs. (2) The high coercivity component was always normal in polarity, which is consistent with emplacement of the Mount Stuart batholith at the end of the Cretaceous long normal. (3) Sites from the batholith and the contact aureole gave similar directions. (4) The directions show no indication of tilt-related smearing. After restoration, the paleomagnetic data indicate $42° \pm 11°$ clockwise rotation and 3100 ± 600 km of northward offset ($\pm 95\%$ confidence). This result verifies Beck et al.'s original interpretation that the Mount Stuart batholith originated at the paleolatitude of northern Mexico.

INTRODUCTION

Paleomagnetic inclinations measured in a broad variety of Late Cretaceous (ca. 100–70 Ma) igneous and sedimentary rocks from the northwest Cordillera are significantly shallower than those predicted using the North American cratonal reference. These discordant data are considered by some to indicate large-scale (≈ 1000– 3000 km), postmagnetization northward displacement relative to the North American craton during the latest Cretaceous and early Tertiary periods (e.g., Beck and Noson, 1972; Beck et al., 1981; Irving et al., 1985; Umhoefer, 1987; Brandon et al., 1988; Beck, 1989; Oldow et al., 1989; Irving and Thorkelson, 1990; Irving and Wynne, 1990; Garver and Brandon, 1994). Early paleomagnetic studies generally discounted local tilting as an explanation for the discordant data (e.g., Beck et al., 1981; Irving et al., 1985) even though many of the best paleomagnetic data were collected from plutonic rocks for which paleohorizontal was poorly constrained.

The interpretation of large-scale northward displacement has become popularly known as the "Baja British Columbia" (Baja BC) hypothesis (cf. Irving et al., 1985). This hypothesis holds that the western parts of British Columbia and Washington State—an enormous crustal mass some 1500 km long and 500 km wide—were transported northward en masse (see Cowan, 1994, for discussion). The term *Baja BC* highlights both the presumed original location of the offset rocks near present-day Baja California and the possible mode of transport by coast-parallel shear, analogous to the northward motion of Baja California along the San Andreas fault (Packer and Stone, 1974; Umhoefer, 1987; Umhoefer et al., 1989).

The possibility of a far-traveled Baja BC has profound implications for our understanding of tectonic processes and plate interactions along the western margin of the North American Cordillera. As a result, the Baja BC hypothesis has received much critical scrutiny. Many workers have argued that regional geologic constraints do not permit large northward offsets (cf. Price and Carmichael, 1986; van der Heyden, 1992), but these arguments carry some unsupported assumptions about continuity of proposed batholithic belts and the uniqueness of proposed stratigraphic and provenance links. The interpretation of paleomagnetic data from the plutons has been questioned because intrusive bodies and surrounding wall rocks rarely preserve unambiguous paleohorizontal indicators
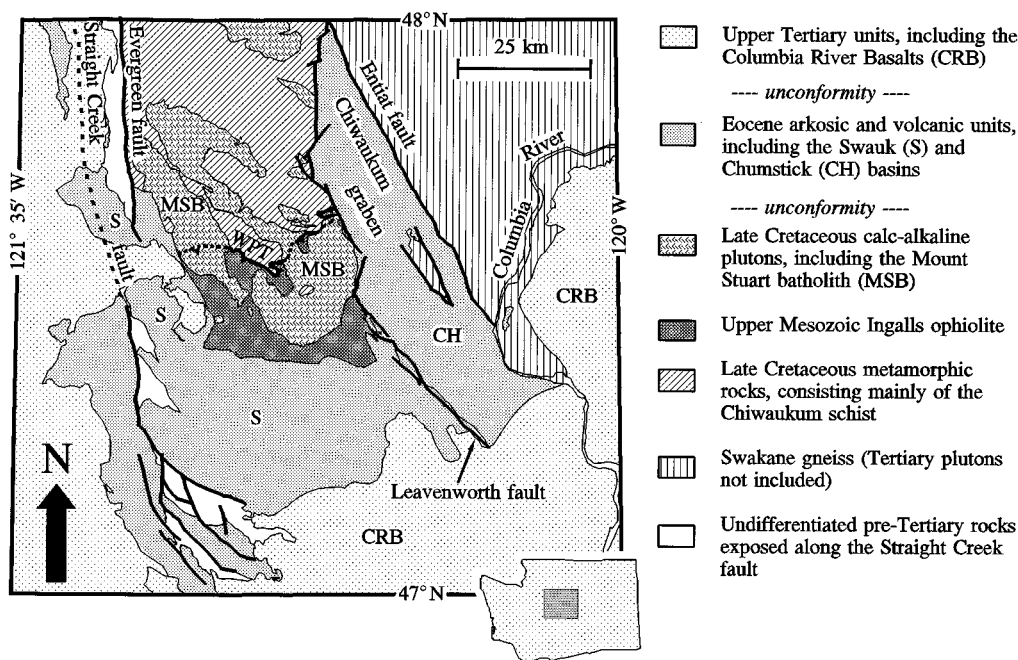
Figure 1. Simplified geologic map of the Mount Stuart area, after Tabor et al. (1982, 1987, 1993) and Frizzell et al. (1984). MSB = Mount Stuart batholith; WPT = Windy Pass thrust; S = Swauk basin; CRB = Columbia River basalts.

(Beck et al., 1981; Irving et al., 1985). For example, Butler et al. (1989) assessed regional structural, metamorphic, and geochronologic relationships and concluded that the discordant paleomagnetic data from the Mount Stuart, Spuzzum, Porteau, Captain Cove, and Stephens Island plutons resulted from postemplacement *tilting* in a down-to-the-southwest sense. Brown and Burmester (1991) came to a similar conclusion based on their study of regional metamorphic gradients around the Spuzzum pluton.

This ongoing debate has prompted new paleomagnetic studies of units where paleohorizontal and the timing of magnetization can be more directly assessed. For example, Wynne et al. (1995) reported paleomagnetic data from bedded sediments and volcanics of the middle Cretaceous Silverquick sediments and Powell Creek volcanics, indicating about 3000 km of postmagnetization northward offset. In our opinion, the paleomagnetic data from plutons remain central to the Baja BC debate because they provide a record from a very different petrologic and thermal setting that can be used to test for regional consistency of the discordant results.

Our contribution to this debate has been the development of a new method based on geobarometry for determining paleohorizontal in granitic batholiths (Ague and Brandon, 1992). Once paleohorizontal at the time of crystallization is determined, primary magnetization directions can be corrected for the effects of postemplacement tilting. The highly discordant paleomagnetic data from the Mount Stuart batholith (Beck et al., 1981), located in the Cascades Mountains of western Washington State, have played a pivotal role in the Baja BC controversy and are the focus of this paper (Fig. 1). Our initial paleohorizontal determinations (Ague and Brandon, 1992) were for the southern part of the batholith because this area coincides with the paleomagnetic sites of Beck et al. (1981). We concluded that the southern part of the batholith was tilted ≈8° in a down-to-the-southeast direction. Restoration of Beck et al.'s (1981) paleomagnetic data according to this tilt indicated

major northward offset of ≈3000 km—a result fully consistent with the Baja BC hypothesis. In this paper, we extend our barometric studies to the entire batholith in order to constrain more precisely its emplacement, tilt, and offset history. As part of this effort, we provide (1) a critical assessment of the aluminum-in-hornblende barometer (Hammarstrom and Zen, 1986) and its application to regional tectonic problems, and (2) a full discussion of the methods used to evaluate paleohorizontal orientation.

REGIONAL GEOLOGIC RELATIONSHIPS

The Mount Stuart batholith (Figs. 2A and 2B) is part of a suite of calc-alkaline plutons that intruded the metamorphic core of the Cascades Mountains during early Late Cretaceous time (Armstrong, 1988; Zen, 1988; Haugerud et al., 1991; Walker and Brown, 1991; Brown and Walker, 1993). The batholith consists mostly of tonalite, quartz diorite, and granodiorite but includes some granite, gabbro, and ultramafite (Fig. 2B) (Pongsapich, 1974; Erikson, 1977, Kelemen and Ghiorso, 1986). For descriptive purposes, the batholith is commonly separated into three parts: an elongate southwest lobe, a hook-shaped region that makes up the northwest part of the northeast lobe, and a bulbous region that makes up the southeast part of the northeast lobe. In this paper, we distinguish between a southern part of the batholith, which is dominated by tonalite and quartz diorite, and a northern part dominated by leucotonalite and biotite granodiorite (Fig. 2B). U/Pb zircon determinations for the Big Jim ultramafic complex and the tonalitic-granodioritic phases of the batholith (Fig. 2B) are ca. 96 and ca. 93 Ma, respectively (Tabor et al., 1982, 1987, 1993; Brown and Walker, 1993; R. B. Miller, 1993, written commun.). K/Ar determinations for biotite-hornblende pairs (Fig. 2B) are mostly concordant and range from ca. 90 to ca. 82 Ma, although one pair from the northeast lobe of the batholith is strongly discordant.
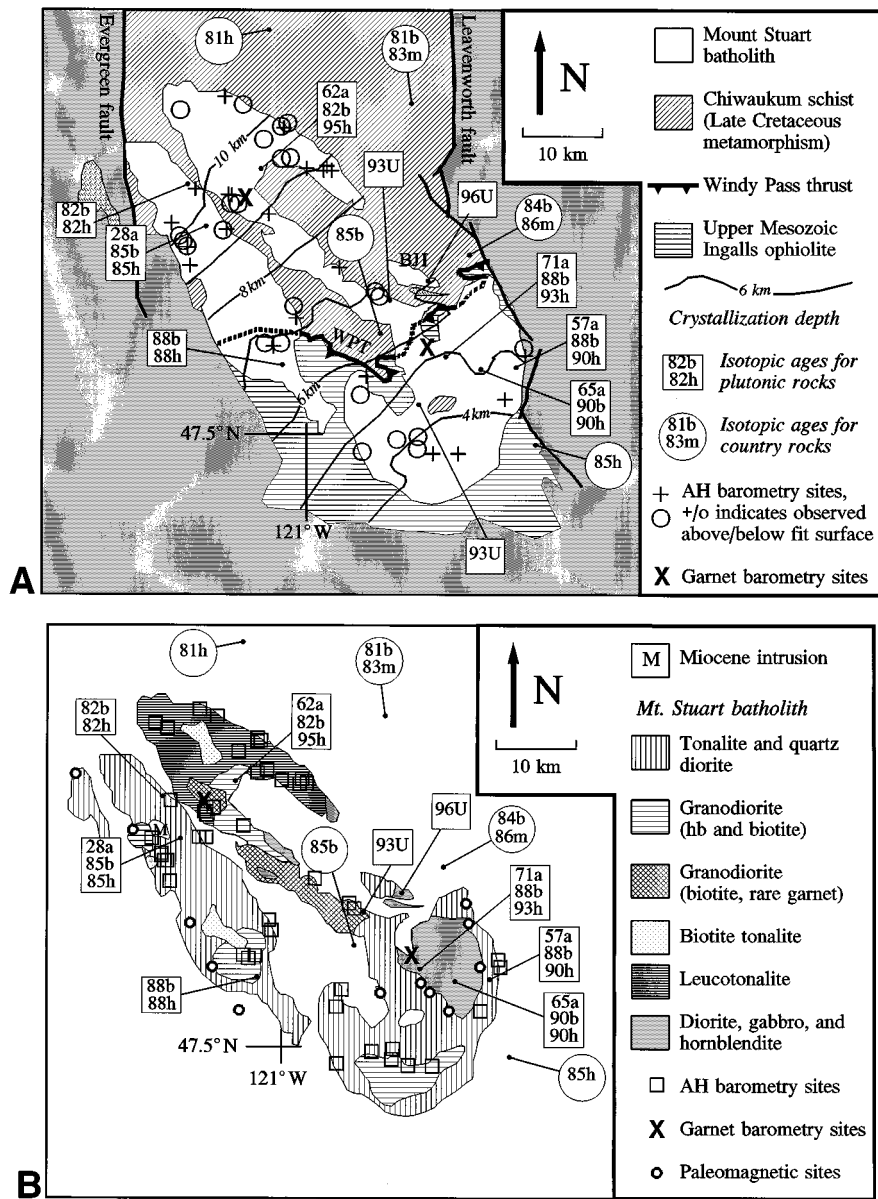
Figure 2. (A) Sample localities, isotopic ages, and depth of crystallization contours for the Mount Stuart batholith area. WPT = Windy Pass thrust; BJI = Big Jim intrusion. Isotopic ages for the Mount Stuart batholith are indicated by boxes, and those for metamorphosed rocks of the Chiwaukum Schist and the Ingalls ophiolite, by circles. U = U/Pb zircon; h = K/Ar hornblende; m = K/Ar muscovite; b = K/Ar biotite; a = apatite fission track ages. Isotopic ages are from Tabor et al. (1982, 1987, 1993), Brown and Walker (1993), and R. B. Miller (1993, written commun.). Contours represent depth of crystallization for the batholith based on the best-fit paleosurface orientation calculated using equation 4 jointly with our aluminum-in-hornblende barometry results. The contours were determined by calculating the intersection of planar isodepth surfaces (isobaric surfaces converted to depth using an average crustal density of 2800 kg m^{-3}) with the present landscape, as represented by 30-second digital topography from the DNAG CD-ROM (National Geophysical Data Center, 1989). (B) Intrusive phases of the Mount Stuart batholith, after Pongsapich (1974) and Erikson (1977), with modifications by Tabor et al. (1982, 1987, 1993) and Frizell et al. (1984).

The Mount Stuart batholith intruded two distinct wall rock units (Fig. 2A), the upper Mesozoic Ingalls ophiolite to the south (Miller, 1985), and the Chiwaukum Schist to the north (Plummer, 1980; Evans and Berti, 1986; Brown and Walker, 1993). The Chiwaukum Schist consists mostly of aluminous pelite with subordinate marble, amphibolite, quartzofeldspathic gneiss, and ultramafite. Ge-

ologic relationships indicate that the Ingalls ophiolite was thrust over the Chiwaukum Schist along a major fault, the Windy Pass thrust, at ca. 95 Ma (Miller, 1985; Evans and Berti, 1986). Because portions of the batholith cut the Windy Pass thrust, intrusion must have occurred, at least in part, after ophiolite obduction (Miller and Paterson, 1992, 1994).

Note error in Figure 3b below: symbols were accidentally switched around in the legend.
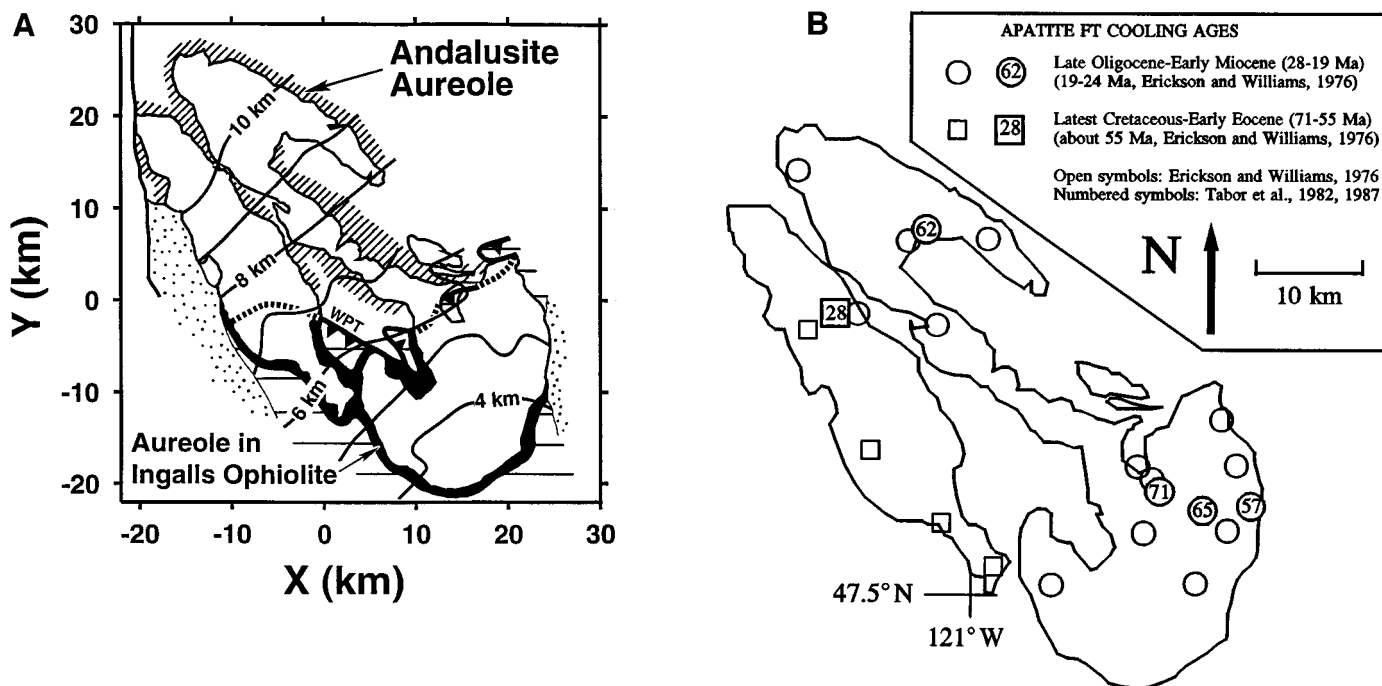

Figure 3. (A) Contact aureole surrounding the Mount Stuart batholith. Andalusite-bearing aureole in Chiwaukum Schist shown with fine diagonal rule; aureole in Ingalls ophiolite shown in black. Depth contours computed from the best-fit paleosurface by determining the intersection of the present topography with surfaces of constant crystallization depth (cf. Fig. 2A). Tertiary rocks = stipple pattern; Ingalls ophiolite = coarse horizontal rule; WPT = Windy Pass thrust (dashed where inferred; cf. Fig. 2A). Aureole extent based on the work of Plummer (1980), Evans and Berti (1986), Brown and Walker (1993), Paterson et al. (1994), and Ague and Brandon (unpubl. field observations). X (east) Y (north) map grid is the same as that used for paleohorizontal estimation; X = 0 and Y = 0 are at long 239°E and lat 47.617°N, respectively. (B) Generalized summary of apatite fission-track ages for the Mount Stuart batholith. The numerical ages of Tabor (1982b, 1987) shown in Figure 2 are supplemented here by general results reported by Erickson and Williams (1976) and Yeats (1977). The Miocene apatite fission-track ages are attributed to heating associated with the intrusion of the Miocene Snoqualamie batholith, which lies directly west of the batholith. The Eocene ages, which characterize the bulk of the batholith, reflect cooling and erosional unroofing following Late Cretaceous plutonism and metamorphism.

The Mount Stuart batholith produced a contact aureole in the surrounding Ingalls ophiolite and Chiwaukum Schist (Frost, 1975; Evans and Berti, 1986; Brown and Walker, 1993). The batholith was almost certainly emplaced at relatively shallow crustal levels, for the aureole in the Chiwaukum Schist contains widespread andalusite (Fig. 3). Around the northeastern margin of the batholith, the aureole was overprinted by amphibolite facies regional metamorphism. Evans and Berti (1986) and Brown and Walker (1993) presented textural evidence that demonstrates that an early generation of andalusite was replaced by kyanite and staurolite in the area directly adjacent to the batholith. In the northeastern part of the Mount Stuart area, metamorphic pressures reached 0.6–0.7 GPa (6–7 kbar; 20–25 km depth) during this younger regional metamorphic event (Evans and Berti, 1986; Brown and Walker, 1993).

The following relationships establish the relative timing of regional metamorphism and ophiolite emplacement. First, the Mount Stuart batholith intruded both the Chiwaukum Schist *and* the Ingalls ophiolite. Second, the presently exposed parts of the batholith must have been emplaced at low pressures because andalusite and relict andalusite occur throughout the contact aureole in the Chiwaukum Schist. Third, replacement textures of kyanite and staurolite after andalusite indicate that regional metamorphism postdated formation of the contact aureole. Biotite and muscovite K/Ar ages for the

Chiwaukum Schist indicate postmetamorphic cooling ca. 82–84 Ma (Fig. 2B). Exhumation following regional metamorphism was rapid. Evans et al. (1993) estimated rates of 5–6 km/m.y. The tectonic significance of this loading/exhumation event is controversial. Evans and Berti (1986) and McGroder (1991) have argued that loading resulted from emplacement of high-level thrust sheets. The alternative hypothesis, magmatic-loading as proposed by Brown and Walker (1993), accounted for the increase in metamorphic pressure by the emplacement of a higher-level batholith.

Apatite fission-track dating (Fig. 3B) shows that by early Eocene time, much of the batholith had cooled to temperatures <100 °C. Assuming a normal thermal profile, these fission track data indicate that present exposures of the batholith have been within ≈3 km of the Earth's surface since the early Eocene. The early Miocene apatite fission-track ages along the southwest margin of the batholith are attributed to heating associated with the intrusion of late Cenozoic plutons to the west of the batholith. A small Miocene stock in the southwest lobe (Erikson, 1977; Fig. 2B) demonstrates the proximity of this younger magmatic activity.

The southwestern margin of the batholith is in contact with southwesterly dipping clastic strata of the lower Eocene Swauk Formation. The nature of this contact—whether stratigraphic or structural—remains unresolved despite considerable debate (see Butler

et al., 1989; Miller et al., 1990; Umhoefer and Magloughlin, 1990; Tabor et al., 1993; Fig. 2A). However, to the south of the batholith, the Swauk Formation clearly rests in angular unconformity on the underlying Ingalls ophiolite (Fig. 2A). Where mapped, this unconformity generally dips to the south (Tabor et al., 1982, 1993; Frizzell et al., 1984).

Butler et al. (1989) argued that regional tilting of the Swauk Formation as exposed along the southwest margin of the batholith indicated post-emplacement tilting of the entire batholith by ≈30° in a down-to-the-southwest direction, enough to fully account for the observed paleomagnetic discordance. This interpretation, however, was based on only a small and poorly exposed area (Miller et al., 1990). For example, most of the Swauk, exposed to the south of the Ingalls ophiolite (Fig. 1), has a general southerly dip, a relationship that is inconsistent with the tilting inferred by Butler et al. (1989). Moreover, throughout the Mount Stuart area, the Swauk strata are generally highly deformed into long-wavelength folds with limb dips of ≈20°–80° (Tabor et al., 1982, 1993; Frizzell et al., 1984). Because the basement to the Swauk (Ingalls ophiolite) shows no evidence of this folding, we conclude that, in many areas, the Swauk has been detached from its basement and folded above decollement-style faults. As a consequence, local bedding orientation is not a useful indicator of paleohorizontal for the batholith.

METHODS FOR PALEOHORIZONTAL ESTIMATION AND STATISTICAL ANALYSIS

Paleohorizontal Estimation

Given reliable measurements of crystallization pressures across the area of a coherent batholith, we can estimate the orientation of paleohorizontal (Ague and Brandon, 1992) by

$$Z_{Tot} = Z/\cos\beta + Z_E = a_0 + a_1 x + a_2 y. \tag{1}$$

Z_{Tot} is the vertical distance from present sea level to the land surface at the time of crystallization (the paleosurface), Z is the depth of crystallization, Z_E is the sample elevation, β is the dip angle of the paleosurface, and a_i are fit coefficients to be determined by least-squares (Fig. 4). β is related to the fit coefficients by

$$\beta = \arctan \sqrt{a_1^2 + a_2^2}. \tag{2}$$

Z is related to crystallization pressure, P, by

$$Z = \frac{P}{\rho g}, \tag{3}$$

where g is the acceleration of gravity, and ρ is the average crustal density, assumed here to be 2800 kg m^{-3}. Rearrangement of equation 1 to isolate Z yields

$$Z = (a_0 + a_1 x + a_2 y - Z_E) \cos\beta = \frac{P}{\rho g}. \tag{4}$$

The objective of our analysis is to use the least-squares method to estimate the fit coefficients in equation 4 based on an observed set of paleodepth measurements, Z_j^{obs}, determined at sample localities (x_j, y_j), where $j = 1, \ldots, n$. The degree of fit is given by

$$\chi^2(a_i) = \sum_j \left(\frac{Z_j^{obs} - Z_j^{calc}(a_i)}{s_j} \right)^2, \tag{5}$$
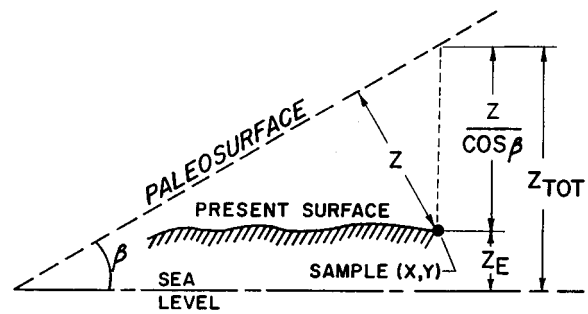
Figure 4. Geometry of the least-squares problem used to estimate paleohorizontal orientation. View is perpendicular to the strike of the paleosurface. For a given sample located at map coordinates (x, y), Z is the depth of crystallization estimated using barometry, Z_E is the sample elevation with respect to present sea level, β is the dip of the paleosurface with respect to present sea level, and Z_{Tot} is the vertical distance from present sea level to the paleosurface.

where Z_j^{calc} is determined from equation 4, and s_j is the standard error for Z_j^{obs}. The best-fit solution corresponds to the set of a_i that minimizes χ^2. This inverse problem is nonlinear and thus must be solved iteratively. For the purposes of fitting, the expected value of s_j is assumed to be approximately constant from sample to sample. Therefore, we do not have to specify s_j to determine the best-fit parameters.

The use of equation 1 to restore paleomagnetic data is based on two major assumptions. The first is that the batholith underwent no significant tilting until after it had cooled through the magnetic blocking temperature (≈200–680 °C; Irving et al., 1985; Beck, 1991). Departures from this assumption can be effectively minimized by using paleomagnetic data from the shallowest and most quickly cooled portions of batholiths (Beck, 1991), which can be readily identified using aluminum-in-hornblende (AH) barometry. The second major assumption is that isobaric surfaces in the cooling magma were parallel to the paleohorizontal. Topographic variation of the landscape over the batholith could introduce horizontal gradients in the pressure field, which would result in a discordance between isobaric surfaces and paleohorizontal. This potential discordance is probably insignificant for our purposes for two reasons. First, the fluid character of the magma would provide little means for supporting lateral "pressure" gradients during crystallization. Second, the local topographic relief was likely to be small. Across modern continental arcs such as the Andes, local changes in elevation are generally <1–3 km over horizontal distances on the order of 100 km (e.g., Grow and Bowin, 1975).

Uncertainty Analysis

In order to properly evaluate our results and their implications for the Baja BC hypothesis, we need to combine uncertainties from our AH barometry with those for estimates of the paleopole position of both the Mount Stuart batholith and the North American cratonal reference frame. The standard statistical methods used in paleomagnetic studies, such as Fisher statistics (Fisher, 1953), do not directly account for errors in paleohorizontal orientation and also are optimized for ease of calculation. Ague and Brandon (1992) used the nonparametric bootstrap method for estimation of uncer-

tainties for the pluton paleomagnetic problem. Relative to conventional paleomagnetic data reduction, our method yields nearly identical values of average terrane displacement and rotation but provides more precise estimates of the uncertainties (or "error brackets") for the average values. The bootstrap calculation provides a more complete account of analytical uncertainties and avoids the systematic biases that arise when a true sample distribution is approximated by an idealized Fisher distribution. Tauxe et al. (1991) outlined the application of the bootstrap method to the analysis of paleomagnetic directions. The reader is referred to Efron (1982) and Efron and Tibshirani (1993) for general information about the bootstrap method and to Tichelaar and Ruff (1989) and Ague (1994) for other examples of its application to problems in the earth sciences. A more extended discussion of the methods used in this paper and by Ague and Brandon (1992) will be presented in a separate contribution.

SAMPLES, ANALYTICAL METHODS, AND STRUCTURAL FORMULA CALCULATIONS

We have made estimates of crystallization pressure using AH barometry at a total of 46 sites throughout the Mount Stuart (Fig. 2A). These comprise 26 sites from Ague and Brandon (1992) and 20 new sites. Equilibration temperatures were estimated for 10 representative samples using amphibole-plagioclase thermometry (Holland and Blundy, 1994). To place additional constraints on the regional pressure regime, we have done TWEEQU thermobarometry (Berman, 1991) on two garnet-bearing rocks collected from within the Mount Stuart batholith: (1) a granite and (2) a gneissic metamorphic screen enclosed by quartz diorite. Sample locations and average compositions of mineral rims are given in Appendix Tables A1–A3.

Mineral composition determinations and back-scattered electron images were obtained using the fully automated JEOL JXA-8600 microprobe at Yale University. Accelerating voltage and beam current were 15 kV and 20 or 25 nA, respectively. Quantitative analyses used natural and synthetic standards, wavelength dispersive spectrometers, offpeak background corrections, and ZAF matrix corrections. Feldspars and micas were analyzed using a slightly defocused (5 μm diameter) electron beam to prevent alkali volatility; analyses of all other phases were done with a focused beam. Compositions in Tables A2 and A3 are averages of 8 to 16 individual "spot" analyses of the rims of two to five grains of the specified mineral in each probe mount.

Structural formulas for all phases except hornblende were calculated assuming that all Fe is divalent. Hornblende structural formula calculations should consider Fe^{2+} and Fe^{3+}, because hornblende can contain significant Fe^{3+}. Following Cosca et al. (1991), we estimated hornblende Fe^{2+} and Fe^{3+} using a structural formula normalization scheme based on Si + Ti + Al + Fe + Mn + Mg = 13 cations per 23 oxygens. The average estimated $Fe^{3+}/(Fe^{3+} + Fe^{2+})$ for our Mount Stuart data set is 0.27 ± 0.077 ($\pm 1\sigma$ sample standard deviation). We note that these estimates of Fe^{2+} and Fe^{3+} are fairly imprecise (Hammarstrom and Zen, 1986; Cosca et al., 1991), but the effect of these uncertainties on AH barometry is very small (≈ 0.01 GPa; Ague and Brandon, 1992).

ALUMINUM-IN-HORNBLENDE BAROMETRY

Both field and experimental studies have shown that in the presence of the appropriate buffer assemblage, the total Al content of hornblende is a sensitive linear function of crystallization pressure (Hammarstrom and Zen, 1986; Hollister et al., 1987; Johnson and Rutherford, 1989; Schmidt, 1992, 1993). Hornblende Al content will also vary as a function of temperature (Spear, 1981; Hammarstrom and Zen, 1986; Holland and Blundy, 1994; Anderson and Smith, 1995). The success of the barometer depends on correctly accounting for these temperature effects; we return to this topic below.

The AH barometer records pressures at or very near the time of magma solidification. The maximum temperature for barometer equilibration is near the solidus, because the full buffering assemblage required for barometry, including quartz and K-feldspar, becomes stable only near solidus conditions. The minimum temperature is governed by the kinetics of the Al exchange reactions. Because of the sluggishness of Al diffusion in chain silicates, the barometer is unlikely to equilibrate at temperatures less than about 650 °C (cf. Freer, 1981; Hammarstrom and Zen, 1986).

The field-based calibrations of the AH barometer by Hammarstrom and Zen (1986) and Hollister et al. (1987) are virtually identical to the experimental calibration by Schmidt (1992). In contrast, the experimental calibration by Johnson and Rutherford (1989) yields pressures that, for a given hornblende Al content, are ≈ 0.1–0.15 GPa lower than those predicted by the other studies. This discrepancy is attributed to the fact that the Johnson and Rutherford (1989) study was done at temperatures ≈ 100 °C higher than solidi for typical granitic magmas using CO_2-rich fluids that are not representative of magmatic fluids (Schmidt, 1992).

In our study, we are most concerned with the *gradient* in the paleopressure field. Consequently, the relative precision, not the absolute accuracy, of the individual pressure determinations is what limits the accuracy of our tilt estimates (Ague and Brandon, 1992). We note that the published calibration curves for Al^T versus P do vary in their absolute position but otherwise have very similar slopes dAl^T/dP. Because dAl^T/dP is the parameter relevant for our study of paleopressure gradients, determinations of paleohorizontal are largely independent of the calibration used (Ague and Brandon, 1992). We use the AH barometer calibration of Schmidt (1992),

$$P = 0.476Al^T - 0.301, \qquad (6)$$

where P is pressure in GPa, and Al^T is the total Al content of hornblende.

The empirical correlation between hornblende Al content and crystallization pressure has been clearly demonstrated, but the use of this relationship as a barometer remains controversial, largely because the specific pressure-sensitive reactions have not been unambiguously identified. Nonetheless, experimental studies (Johnson and Rutherford, 1989; Schmidt, 1992) strongly suggest that the pressure-sensitive change in hornblende Al content is governed by the *tschermak* exchange: $(Mg, Fe^{2+})_{-1}Al^{VI}Al^{IV}Si_{-1}$. In other words, increases in Al content with pressure arise from equal amounts of substitution of Al^{IV} for Si on tetrahedral sites and Al^{VI} for Mg, Fe^{2+} on octahedral sites. Hollister et al. (1987) proposed a reaction that may govern the *tschermak* exchange for calc-alkaline magmas, but it has not been rigorously tested.
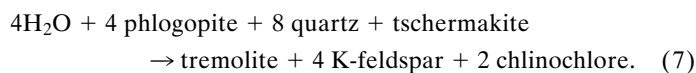
Practical Application of the AH Barometer

Practical application of the barometer requires attention to several issues.

Critical Mineral Assemblage Required for Barometry. As discussed in all field and experimental calibration studies of the AH barometer, pressure determinations must be done on samples that contain hornblende in textural equilibrium with biotite, K-feldspar, quartz, plagioclase, sphene, and Fe-Ti oxides. For the Mount Stuart samples, the macroscopically observable oxide phase is ilmenite. Experience indicates that pressure estimates for rocks that lack K-feldspar are systematically too high relative to those where the full critical assemblage is present (Ague and Brimhall, 1988). Our results were obtained by analyzing the rims of euhedral hornblende crystals coexisting with the full buffer assemblage required for barometry. In this way, we maximize the probability that the hornblende composition reflects chemical equilibrium among all phases of the required critical assemblage. Schmidt (1993) gives a detailed discussion of the importance of the phase assemblage in controlling hornblende Al content.

Anderson and Smith (1995) and Paterson et al. (1994) have also reported AH barometry results for the Mount Stuart batholith. We have not considered their results in our analysis, because these workers failed to ensure that the critical assemblage was present in those samples used for pressure estimation. In particular, their sample suite included K-feldspar–absent tonalites and quartz diorites.

Oxygen Fugacity. Ague and Brimhall (1988) found that pressure estimates from Fe-rich amphiboles (log $[Mg/Fe^{Total}] < \approx -0.2$) that crystallized under very low f_{O2} conditions were systematically too high. Anderson and Smith (1993) came to a similar conclusion, and suggested that the effect was because of ". . . low Mg no longer competing with Al^{VI} for occupancy of the M2 site." This problem does not affect our results, because the Mount Stuart amphiboles are fairly Mg-rich (Table A2; Pongsapich, 1974).

Low-Temperature Alteration. Hammarstrom and Zen (1986) pointed out that low-temperature subsolidus alteration of hornblende could result in erroneous pressure estimates. A common example is the late-stage alteration of hornblende rims to actinolite. Actinolitic alteration, if undetected, will result in anomalously low pressure estimates. Back-scattered electron (BSE) imaging is a powerful tool for determining alteration in hornblende, especially if used in high-contrast mode. For example, two BSE images of the same amphibole are shown in Figure 5. One (Fig. 5A) was taken using standard operating conditions, whereas the other (Fig. 5B) was taken using high-contrast mode. Alteration features along cracks and grain boundaries are immediately apparent in the high-contrast photo. Similar BSE imaging tests were done on all of our Mount Stuart samples; those whose hornblendes showed extreme compositional variations and alteration along microcracks and cleavages were rejected. Subsolidus production of Al-poor amphibole is typically associated with chloritization of biotite, which suggests alteration reactions of the form

$$4H_2O + 4 \text{ phlogopite} + 8 \text{ quartz} + \text{tschermakite}$$
$$\rightarrow \text{tremolite} + 4 \text{ K-feldspar} + 2 \text{ chlinochlore.} \quad (7)$$

Note that alteration features are generally rare, except in the region overprinted by regional metamorphism in the northern part of the batholith.
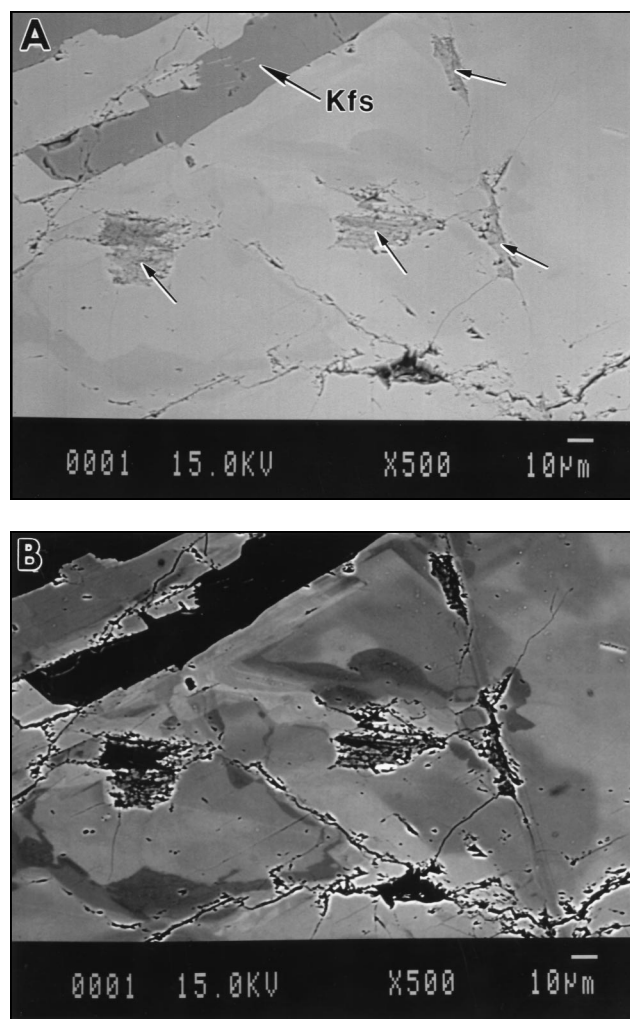
Figure 5. Back-scattered electron (BSE) images of subsolidus alteration of hornblende. (A) Normal-contrast image. Ksp is K-feldspar in contact with the hornblende rim, and the arrows point to small inclusions of chloritized biotite within the hornblende. (B) High-contrast image. Variations in gray scale indicate variations in hornblende composition. Dark gray areas are actinolitic hornblende with high Mg/Fe and Si/Al, whereas light gray areas are more aluminous hornblende with significantly lower Mg/Fe and Si/Al. The considerable compositional variations along cracks and near chloritized biotite inclusions is interpreted to reflect fluid-driven subsolidus alteration.

Temperature Dependence of Hornblende Al^T. The total Al content of hornblende Al^T is a function of both temperature and pressure (Spear, 1981; Hammarstrom and Zen, 1986; Blundy and Holland, 1990; Holland and Blundy, 1994). Increases in temperature promote edenite-type substitutions, which enrich hornblende in Al^{IV} but not Al^{VI} (Holland and Blundy, 1994; Anderson and Smith, 1995). As a result, if the AH barometer assemblage equilibrates at temperatures that differ greatly from the conditions of barometer calibration, then pressure estimates will be in error (Anderson and Smith, 1995).

In principle, independent mineral thermometers could be used to assess the effects of equilibration temperature on AH barometry.

Anderson and Smith (1995) and Paterson et al. (1994) attempted to do this for a variety of calc-alkaline intrusions, including the Mount Stuart batholith, using the hornblende-plagioclase thermometer of Blundy and Holland (1990). Anderson and Smith (1995) and Paterson et al. (1994) noted a positive correlation between estimates of pressure and temperature and suggested that the barometer was giving biased pressure estimates because of temperature sensitivity.

Although temperature effects can influence hornblende Al content, one must view the temperature estimates of Anderson and Smith (1995) and Paterson et al. (1994) with caution. As discussed by Mengel and Rivers (1991) and Holland and Blundy (1994), the Blundy and Holland (1990) thermometer is flawed and is incompatible with a broad spectrum of amphibole compositions. For example, the Blundy and Holland (1990) thermometer tends to overestimate equilibration temperature for hornblendes with X_{Al}^{M2} (= $Al^{VI}/2$) in excess of $\approx$0.15–0.2 such that the error increases systematically as X_{Al}^{M2} increases (see Figure 1 of Holland and Blundy, 1994). Conversely, the thermometer may underestimate temperature for less aluminous amphiboles. Because hornblende coexisting with the AH barometer assemblage will show a systematic increase in X_{Al}^{M2} with pressure, the flaws in the Blundy and Holland (1990) thermometer will tend to produce an artificial positive correlation between estimates of crystallization temperature and pressure. Although Anderson and Smith (1995) acknowledged the problems with the Blundy and Holland (1990) formulation, they argued that the flaws do not significantly affect temperature estimates for metaluminous tonalite and granodiorite bulk compositions.

We can assess independently the performance of the Blundy and Holland (1990) thermometer for the case where plagioclase and hornblende coexist with the AH barometer assemblage by using the tonalite phase equilibrium experiments of Johnson and Rutherford (1989) and Schmidt (1993). One problem with this approach is that the plagioclase and orthoclase compositions for Schmidt's 0.25–0.45 GPa experiments are not equilibrium compositions (J. L. Anderson, 1995, personal commun.). For example, the Fuhrman and Lindsley (1988) two-feldspar thermometer predicts temperatures in excess of $\approx$1000 °C for these experiments, but the known experimental temperatures were $\approx$700 °C. Schmidt (1993) suggested that some of the experimental plagioclase compositions may reflect some type of metastable behavior, but our interpretation is that the plagioclase analyses are in error. Schmidt (1993) noted that the plagioclase that crystallized during the experiments grew as rare, thin ($<$5 μm) rims on seed crystals. Because Schmidt (1993) used a slightly defocused electron beam to analyze the run products, it seems likely that the problematic plagioclase compositions represent a mixture of the compositions of the thin rim overgrowths and the starting seed crystals. Above 0.45 GPa, Schmidt's (1993) coexisting feldspar compositions are reasonably consistent with experimental temperatures and apparently were not affected by this problem.

In contrast to plagioclase, orthoclase compositions do not appear to be complicated by experimental or analytical problems (Schmidt, 1993). Therefore, we estimated the plagioclase compositions in equilibrium with the measured orthoclase compositions for the 0.25–0.45 GPa experiments of Schmidt (1993) using the activity-composition relationships for the ternary feldspars derived by Fuhrman and Lindsley (1988). Using equation 11 of Fuhrman and Lindsley (1988), the computed equilibrium X_{Albite} values for plagioclase are 0.79, 0.80, and 0.75 for the 0.25, 0.35, and 0.45 GPa experiments of Schmidt (1993), respectively. These plagioclase compositions were used for the temperature estimates described below.
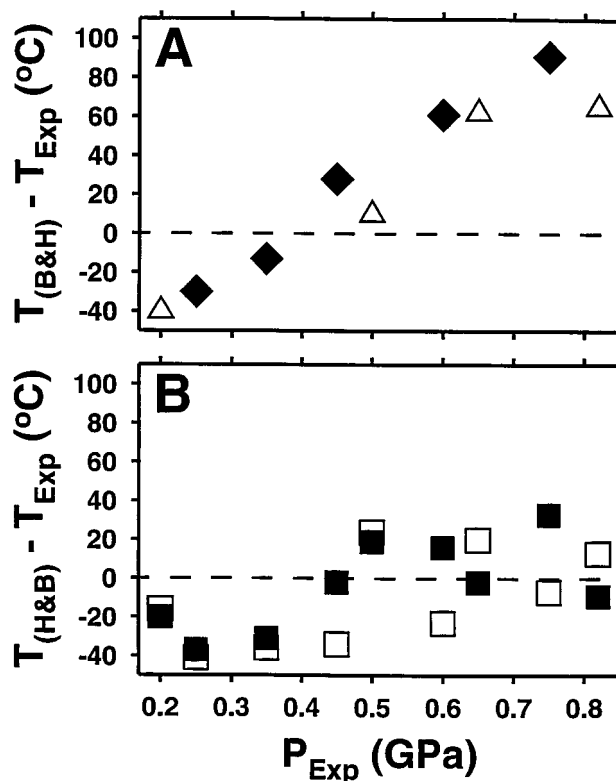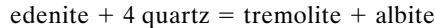

Figure 6. Comparison of amphibole-plagioclase thermometers using the tonalite phase equilibrium experiments of Johnson and Rutherford (1989) and Schmidt (1993). (A) Blundy and Holland (1990) thermometry. $T_{(B\&H)}$ is temperature calculated with the Blundy and Holland (1990) thermometer, T_{Exp} is the actual experimental temperature, and P_{Exp} is the experimental pressure. Open triangles denote experiments FC78, FC106, FC129, and FC119 of Johnson and Rutherford (1989; a summary of the feldspar compositions and temperatures for these experiments is provided by Holland and Blundy, 1994). Filled triangles = experiments of Schmidt (1993). Note that there is an artificial positive correlation between temperature estimates and experimental pressures. (B) Temperatures of equilibration for the experiments described in Figure 6A computed using thermometers A (open squares) and B (filled squares) of Holland and Blundy (1994). $T_{(H\&B)}$ is temperature calculated using the Holland and Blundy (1994) thermometers, and T_{Exp} is the actual experimental temperature. In general, the Holland and Blundy (1994) thermometers perform much better than the earlier Blundy and Holland (1990) thermometer.

The performance of the Blundy and Holland (1990) thermometer for the experimental data of Johnson and Rutherford (1989) and Schmidt (1993) is shown in Figure 6. For the pressure range of interest ($<$$\approx$0.8 GPa), the estimated temperatures and the known experimental pressures of Johnson and Rutherford's and Schmidt's experiments are positively correlated (Fig. 6A). The correlation is entirely artificial and is the result of temperature underestimation at pressures below $\approx$0.35 GPa and temperature overestimation at higher pressures. The amount of error can be large, ranging from $-$40 to $+$90 °C between $\approx$0.2 and $\approx$0.8 GPa. On this basis we conclude that the positive correlation between AH pressure estimates
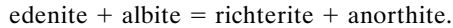
and Blundy and Holland (1990) temperature estimates discussed by Anderson and Smith (1995) results largely from errors in the Blundy and Holland (1990) calibration. It follows that the temperature "corrections" to AH pressure estimates made by Anderson and Smith (1995) using the Blundy and Holland (1990) thermometer are suspect.

Holland and Blundy (1994) recognized the flaws in the earlier Blundy and Holland (1990) thermometer and presented two new thermometer calibrations that incorporate nonideal mixing models for amphibole. The thermometer reactions are

$$\text{edenite} + 4\,\text{quartz} = \text{tremolite} + \text{albite}$$

and

$$\text{edenite} + \text{albite} = \text{richterite} + \text{anorthite}.$$

When applied to the experimental data of Johnson and Rutherford (1989) and Schmidt (1993), the Holland and Blundy (1994) thermometers perform somewhat better than the Blundy and Holland (1990) thermometer, particularly at pressures in excess of ≈ 0.4 GPa (Fig. 6B). The temperature estimates are accurate to within $\pm 50\,°C$ (Fig. 6B). A weak positive correlation between pressure and Holland and Blundy (1994) temperature estimates is apparent, but the slope of the trend is significantly smaller than that observed for the Blundy and Holland (1990) temperature estimates (cf. Fig. 6A).

THERMOBAROMETRY RESULTS

Aluminum-in-Hornblende Barometry

Pressure estimates determined using AH barometry decrease from ≈ 0.3 to ≈ 0.15 GPa from northwest to southeast (Fig. 7A). The northwest-southeast trend is maintained regardless of rock type (granite, granodiorite, or tonalite; see Fig. 2B), which suggests that bulk rock composition has little effect on the pressure estimates. The pressure estimate for one sample at the northern tip of the batholith (MS-275) is anomalously high (≈ 0.47 GPa) and was not included in the paleohorizontal analysis. This sample is from the area overprinted by regional metamorphism, but metamorphic temperatures (500–600 °C; Evans and Berti, 1986; Brown and Walker, 1993) were probably not high enough to reset hornblende compositions in the absence of a fluid phase (Hammarstrom and Zen, 1986). Fluid-driven alteration of hornblende would be expected to produce significant alteration textures along cracks and grain boundaries (Fig. 5B), but these were not observed. It is possible that MS-275 is from a part of the intrusion that was still crystallizing during regional metamorphism and deep burial of the northeastern part of the batholith. If this interpretation is correct, then such late-stage magmatism would seem to be very local in that it is observed at only one of our sample sites.

Thermobarometry of Garnet-Bearing Rocks Within the Batholith

Thermobarometry was done on two garnetiferous samples from within the batholith in order to place additional constraints on emplacement pressures. Pressure-temperature (P-T) estimates were made using the TWEEQU software of Berman (1991). Activity-composition relations for garnet, biotite, muscovite, and plagioclase were computed using the models recommended by Berman (1991) and McMullin et al. (1991). Ideal mixing was assumed for K-feldspar, and quartz was taken to be pure. Rim compositions of phases in mutual contact were used for P-T estimation.
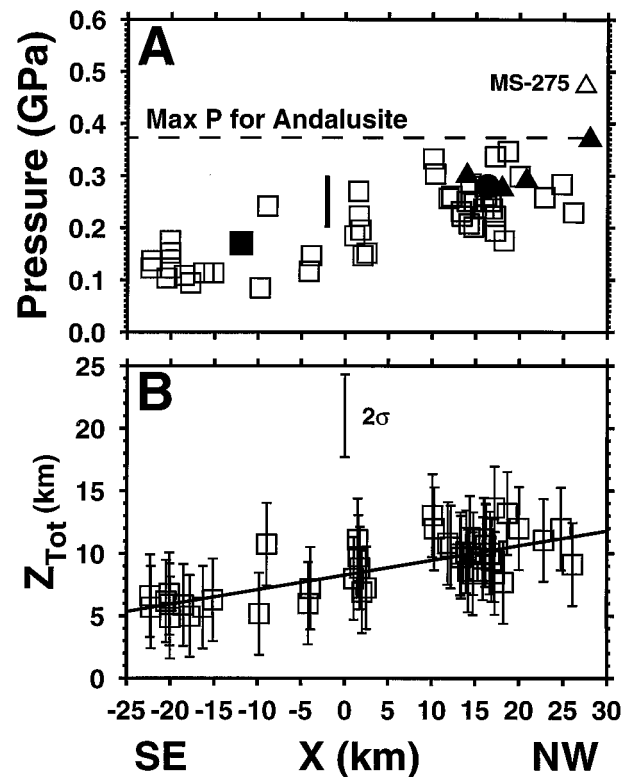

Figure 7. (A) View perpendicular to the strike of the reconstructed paleosurface (see text and Fig. 4), illustrating pressure determinations across the batholith. NW and SE denote the map directions northwest and southeast, respectively. Heavy vertical bar = contact metamorphosed peridotites of Paddy-Go-Easy Pass (Frost, 1975); filled triangles = Chiwaukum Schist in the Mount Stuart aureole (Sample 4 of Evans and Berti, 1986; Samples 172-36a, 173-180a, and 173-254i of Brown and Walker, 1993). The contact metamorphism pressure quoted for 172-36a was computed by Brown and Walker using garnet core compositions (see Fig. 8 in Brown and Walker, 1993). Open squares = AH barometry sites; filled circle = MS-210; filled square = MS-305. Note general decrease in pressure from ≈ 0.3 GPa in the northwest to ≈ 0.15 GPa in the southeast. (B) View perpendicular to the strike of the reconstructed paleosurface, illustrating the individual data points used in the least-squares fitting procedure (compare with Fig. 4). The best-fit paleosurface is indicated by the solid line. The expected variation for each datum ($\pm 2\sigma$) is denoted by the error bars.

The first sample is a garnetiferous, two-mica granite from the northern part of the batholith (MS-210; Fig. 2A). Fluid-absent equilibria involving muscovite, K-feldspar, biotite, plagioclase, quartz, and garnet yield a P-T estimate of 0.28 ± 0.05 GPa and $510 \pm 38\,°C$ (1σ TWEEQU uncertainties; see Berman, 1991). Our AH barometry results predict a nearly identical pressure of about 0.3 GPa for this location.

The second sample is from a screen of coarsely crystalline plagioclase + quartz + biotite + garnet + K-feldspar + cordierite gneiss surrounded by quartz diorite in the southern portion of the batholith (MS-305; Fig. 2A). The cordierite is altered to pinnite and is unsuitable for thermobarometry, but the other minerals are fresh. TWEEQU P-T estimates can be calculated for equilibria in-

volving K-feldspar, biotite, plagioclase, quartz, and garnet, if the activity of water is specified. Taking $a_{H_2O}^{Fluid} = 1$ yields a P-T estimate of 0.17 GPa and 706 °C. This is a *maximum* estimate for P; decreasing $a_{H_2O}^{Fluid}$ decreases P estimates. The T estimate is nearly independent of the $a_{H_2O}^{Fluid}$ value used in the calculations. Our AH barometry predicts a pressure of $\approx$0.18 GPa for the MS-305 locality.

The pressure estimates for the garnetiferous samples imply a general decrease in pressure from north to the south-southeast and are in good agreement with the trend defined by AH barometry (Fig. 7A). The high equilibration temperature for MS-305 is appropriate for a strongly recrystallized gneiss engulfed in quartz diorite. The temperature estimated for MS-210 is considerably lower and reflects equilibration under sub-solidus conditions.

**Comparison with Contact Aureole Barometry**

A number of pressure estimates have been published for the contact aureole surrounding the Mount Stuart batholith. Frost (1975) estimated that ultramafic rocks of the Ingalls ophiolite in the Paddy-Go-Easy Pass area along the southwestern margin of the batholith were metamorphosed at pressures of 0.2–0.3 GPa. Our prediction at this locality is $\approx$0.2 GPa based on AH barometry (Fig. 7A). Evans and Berti (1986) and Brown and Walker (1993) estimated pressures of $\approx$0.3 GPa for andalusite- or sillimanite-bearing schists of probable contact metamorphic origin in the north-central Mount Stuart area (Fig. 7A). Our AH barometry results from adjacent plutonic rocks are in the range of $\approx$0.2–0.35 GPa (Fig. 7A). Overall, our AH barometry agrees well with available aureole barometry.

To the south of the batholith, some meta-igneous and meta-sedimentary units of the Ingalls ophiolite far removed from the thermal aureole of the batholith preserve very low-grade, prehnite-bearing mineral assemblages (Miller, 1985). This relationship strongly suggests that the shallowest levels of the batholith are exposed at its southern end, consistent with our AH barometry results.

Effect of Temperature on AH Barometry

Al^{IV} and Al^{VI} Systematics of Hornblende. As discussed above, the pressure-sensitive change in hornblende Al content is probably governed by the *tschermak* exchange. If the *tschermak* substitution governs hornblende Al systematics, then both Al^{VI} and Al^{IV} should increase by the same amount for a given increase in Al^{T}. On the other hand, temperature-sensitive edenite substitutions will enrich hornblende in Al^{IV} but not Al^{VI}. As shown in Figure 8A, our hornblende analyses from the Mount Stuart batholith conform closely to the relationship predicted by the *tschermak* substitution. Moreover, hornblende Al systematics are virtually identical to those observed for the experimental AH barometer calibration studies of Schmidt (1992, 1993; Fig. 8B).

Estimates of Equilibration Temperature. We have estimated equilibration temperatures for 10 representative tonalite and granodiorite samples of the Mount Stuart batholith using Holland and Blundy (1994) thermometry to determine if our AH barometry results could be biased by temperature effects (Table 1 and Fig. 9). The temperature estimates do not vary in any systematic way when plotted against pressure determined using the AH barometer (Fig. 9A). The average of the estimated temperatures is $\approx$650 °C (Fig. 9B). We attribute much of the scatter in calculated tempera-
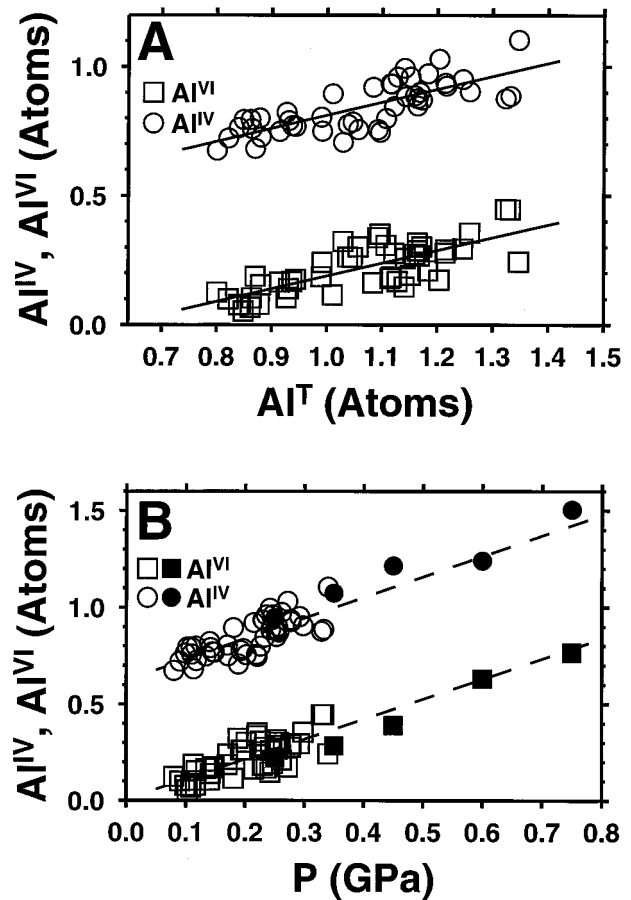
Figure 8. Compositional systematics for the Mount Stuart batholith hornblendes. Pressures estimated using the Schmidt (1992) calibration of the aluminum-in-hornblende (AH) barometer. See text for additional discussion. (A) Mount Stuart hornblende Al^{VI} and Al^{IV} as functions of total Al content (Al^{T}). Linear least-squares regressions denoted by solid lines. Increases in hornblende Al content are governed almost entirely by pressure-sensitive *tschermak*-type substitutions, regardless of Al^{T} value. (B) Hornblende Al^{VI} and Al^{IV} for the Mount Stuart batholith (open symbols) and the experimental AH barometer calibration studies of Schmidt (1992, 1993) (solid symbols) as functions of pressure. Linear least-squares regressions of the Mount Stuart data denoted by dashed lines. Note that the Al systematics for the Mount Stuart samples and the experimental studies are closely comparable.

ture (Fig. 9A) to statistical errors in the structural formula estimates of hornblende Fe^{3+}, Na^{A}, and Na^{M4}.

Analysis. The calculated temperatures are directly comparable to the temperatures of AH barometer calibration (Hammarstrom and Zen, 1986; Hollister et al., 1987; Schmidt, 1992) and strongly suggest that assemblage equilibration occurred at or very near magmatic conditions. Our calculations are fully consistent with the observation that the Al systematics of the Mount Stuart batholith hornblendes are dominated by the pressure-sensitive *tschermak* substitution, regardless of the pressure estimate (Fig. 8). Therefore, we conclude that temperature effects have a negligible influence on our pressure estimates.

We emphasize that even if our pressure estimates were con-

TABLE 1. TEMPERATURE ESTIMATES

Sample	Xab*	Al[T†]	P[§] (GPa)	T_A[#] (°C)	T_B[#] (°C)
MS-003	0.76	0.94	0.14	636	648
MS-028	0.75	0.87	0.11	634	649
MS-103	0.69	1.00	0.17	616	664
MS-112	0.71	1.19	0.26	654	662
MS-131	0.80	1.02	0.18	666	645
MS-171	0.68	1.26	0.29	619	658
MS-206	0.66	1.18	0.26	620	627
MS-275	0.69	1.62	0.46	673	658
WP-454	0.74	0.87	0.11	603	678
WP-545	0.67	1.14	0.24	695	664

*Mole fraction of albite in plagioclase.
[†]Total Al in hornblende.
[§]Pressure computed using the Schmidt (1992) calibration of the AH barometer.
[#]Temperatures computed using plagioclase-hornblende thermometers A and B of Holland and Blundy (1994).

Figure 9. Temperature and pressure of equilibrium for 10 representative Mount Stuart batholith samples computed using amphibole-plagioclase thermometers of Holland and Blundy (1994) and the aluminum-in-hornblende barometer calibration of Schmidt (1992; Table 1). (A) Temperature estimates made using thermometers A (open squares) and B (filled squares) of Holland and Blundy (1994). Error bars correspond to ±40 °C uncertainties for amphibole-plagioclase thermometry given by Holland and Blundy (1994). Mean temperature of ≈650 °C denoted by dashed line. (B) Average temperature estimates for the samples computed by averaging results for thermometers A and B of Holland and Blundy (1994). Mean temperature of ≈650 °C denoted by dashed line. Note lack of correlation between temperature and pressure estimates.

taminated by biases resulting from variations in intensive variables such as temperature outside the range of AH barometer calibration, our estimate of paleohorizontal would be affected only in the case of systematic, batholith-scale gradients in the relevant variables, a case which we consider to be unlikely. More likely are local-scale variations that would appear as random errors in our pressure determinations. These errors would tend to be averaged out in our analysis and thus should have little effect on our determination of pressure gradients at the scale of the entire batholith.

PALEOHORIZONTAL ORIENTATION AND IMPLICATIONS FOR AH BAROMETRY

Paleohorizontal Orientation

Depth contours for Z were computed from the best-fit paleo-surface by determining the intersection of the present topography with surfaces of constant crystallization depth (Figs. 2A and 10). The pattern of the contours reflects the ≈3 km of topographic relief across the Mount Stuart area. The average absolute value of the residuals is only 1.2 km (maximum residual = 3.4 km). The residuals show no systematic pattern in map view and appear randomly disposed above and below the best-fit surface. These results strongly suggest that paleohorizontal is well represented as a simple planar surface. Our analysis indicates that paleohorizontal dips gently to the southeast; the strike and dip of the best-fit surface are 43.2° ± 30.4° and 7.0° ± 2.0° southeast, respectively (±95% confidence; Fig. 7B).

It is useful to calculate separate estimates of paleohorizontal for the southern and northern parts of the batholith, given that these areas may have had separate tilt histories. The southern part has a strike of 55° ± 38° and dip of 8° ± 3° to the southeast. The northeast lobe has a strike of 85° ± 88° and dip of 7° −6/+17° southeast (note that the confidence distribution is non-Gaussian). The large uncertainties associated with the northern part of the batholith (the "hook shaped" portion) reflect the fact that the paleohorizontal surface is poorly constrained because of the restricted sample distribution imposed by the elongate shape of the body. It is important to note, however, that both results indicate a gentle south or southeast dip for the batholith.
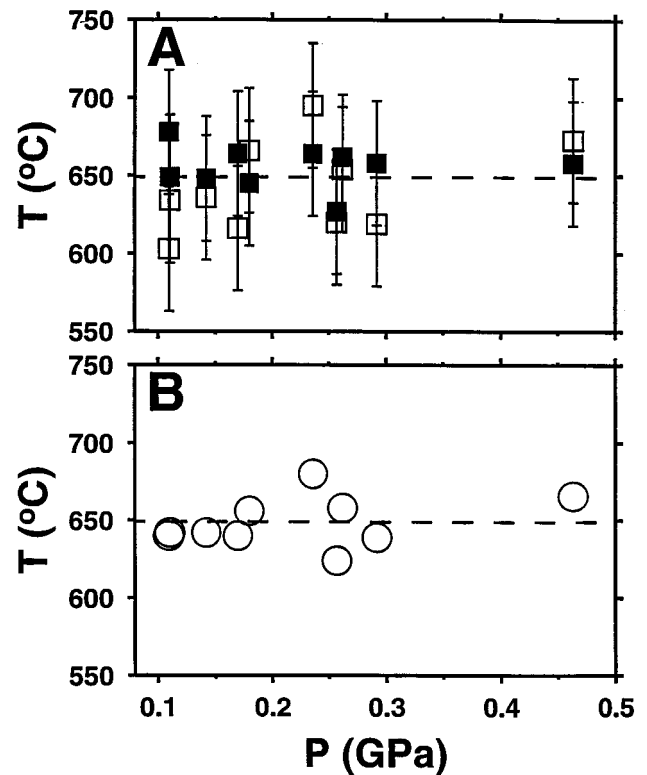
Implications for the AH Barometer

A direct test of the variability inherent in geologic applications of the AH barometer can be made using our data and the planar paleosurface model (equation 4). For the best-fit paleosurface, the observed residuals for the Z_j values have a variation of ≈3.2 km (±2σ) in depth (Fig. 7B), and ≈±0.1 GPa in pressure. This estimated variation is for a *single* pressure estimate. Variability on the order of ±0.1 GPa is comparable to that observed in the experimental calibrations of the AH barometer. Thus, we infer that the natural system is well approximated by the experimental studies. However, we stress again that this low level of variability is attainable only if one uses appropriate samples, namely, those which contain unaltered igneous hornblende in textural equilibrium with the full buffering assemblage required for the barometer.

It is critical to emphasize that the variability of the individual depth determinations (±3.2 km) should not be taken as an indicator of the precision of the tilt estimate. The best-fit tilt estimate is much
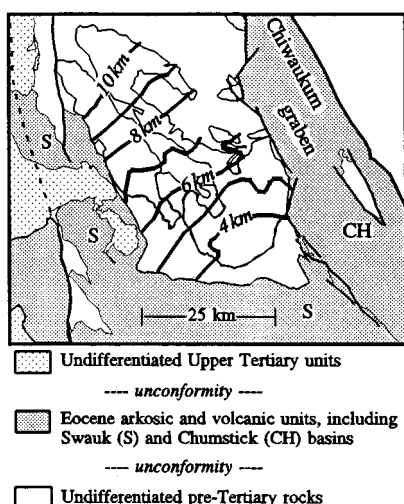
Figure 10. Depth contours computed from the best-fit paleo-surface by determining the intersection of the present topography with surfaces of constant crystallization depth (cf. text and Fig. 2A).

more precise because it is based on all of the depth determinations across the full area of the batholith (see Taylor, 1982, for a discussion of uncertainty versus random variation).

DISCUSSION

Regional Structural and Stratigraphic Relationships

The general stratigraphic succession in the vicinity of the Mount Stuart batholith also bears on the question of regional tilt. From north-northwest to south-southeast across the Mount Stuart area, one moves in an up-section direction from the Chiwaukum Schist through the Ingalls ophiolite into the unconformably overlying sedimentary strata of the Swauk Formation (Figs. 1 and 10). We take these relationships as evidence that, at the regional scale, the Mount Stuart block presently dips gently to the south-southeast, consistent with our results.

The Windy Pass thrust and superjacent Ingalls ophiolite probably originated as a near-horizontal structural sequence that extended across the entire Mount Stuart area. The present southerly dip of the fault (Miller, 1985) and the outcrop pattern of the Ingalls ophiolite (Figs. 1 and 2) are, therefore, compatible with our best-fit tilt estimate. A subtle feature that we call attention to is the fact that the Windy Pass thrust appears to climb from the 7 km contour in the southwest to the 6 km contour in the northeast (Figs. 2A, 3A). Because thrust faults are generally observed to climb in the direction of transport, we interpret this relationship as indicating top-north-east motion on the Windy Pass thrust. This direction is consistent with the cross section reconstructions of McGroder (1991), which show the Ingalls being thrust from the metamorphic core of the Cascades in a top-northeast direction, but is contrary to the top-north interpretation of Miller (1985). Miller's (1985) interpretation was based, in part, on the present southward dip of the Windy Pass thrust, which we have shown is the result of postemplacement tilting of the Mount Stuart area.

Summary of Inferred Sequence of Regional Tilting Events

Now we summarize the tectonic history of the Mount Stuart area, starting with the top-northeast(?) thrusting of the Ingalls ophiolite over the Chiwaukum schist at ca. 96–94 Ma (Miller, 1985). This thrusting was followed by intrusion of the Mount Stuart batholith at ca. 96–93 Ma (Tabor et al., 1982, 1993; Brown and Walker, 1993; R. B. Miller, 1993, written commun.). Our AH barometry demonstrates that the batholith, as presently exposed, was everywhere emplaced at relatively shallow crustal levels (<12 km; Figs. 2A and 3A). The 6–7 km depth for the Mount Stuart batholith in the vicinity of the Windy Pass thrust (Figs. 2A and 3A) indicates that emplacement of the Ingalls thrust sheet caused only modest loading.

Intrusion of the batholith was followed by a second loading event and subsequent rapid exhumation. The second loading is recorded by a metamorphic gradient, increasing to the northeast, with the maximum grade marked by widespread kyanite in the Chiwaukum schist to the north and northeast of the batholith. In this area, the exposed margin of the batholith was driven downward from an initial depth of ≈10 km to a maximum depth of 22 to 25 km—a total burial of 10–15 km (Brown and Walker, 1993). U/Pb ages for metamorphic monazite indicate that peak metamorphism was at 90–88 Ma (Brown and Walker, 1993). K/Ar mica ages record postmetamorphic cooling at ca. 86–82 Ma. The northeast part of the batholith shows clear evidence of having been affected by this load-related metamorphism, as indicated by (1) discordant K/Ar hornblende/biotite ages, (2) regional metamorphic overprinting of the contact aureole (Evans and Berti, 1986; Brown and Walker, 1993), and (3) chloritic alteration of igneous hornblende and biotite in the batholith. Much of the southwestern part of the batholith was apparently not affected, as indicated by (1) tight concordance between K/Ar hornblende/biotite ages, (2) the absence of postintrusion metamorphism of the contact aureole along the southeast margin of the batholith, and (3) well-preserved igneous hornblende and biotite.

These relationships show that the Mount Stuart area was affected by regional-scale tilting in a northeast-down direction (Brown and Walker, 1993). What remains unresolved is how much of the batholith was affected. Tilting may have been confined to the northern part of the batholith, which would imply a fold hinge located between the two lobes of the batholith. On the other hand, the tilting may have involved the whole batholith, which would imply a fold hinge near the southwest margin of the batholith. Resolution of the tilt geometry has an important bearing on the interpretation of the paleomagnetic data, a point we return to below.

A remarkable aspect of this northeast-down tilting is that it was nearly completely reversed during postmetamorphic exhumation. This conclusion is supported by the following observations: (1) the batholith is presently surrounded on all sides by an originally shallow contact aureole (Fig. 3A), (2) the isodepth surfaces determined from the AH barometry appear to share a common planar attitude throughout the batholith (Figs. 7 and 10), and (3) apatite fission-track ages indicate that, by early Eocene time, the presently exposed level of the batholith was within 3 km of the surface (Fig. 3B).

The cycle of tilting and untilting described above seems too coincidental to have happened by chance alone. We suggest that loading was caused by emplacement of a tapered thrust sheet that decreased in thickness to the south-southeast (e.g., "supra-Nason" thrust sheet of McGroder, 1991). To account for the observed kyanite overprint, the thrust sheet would have to have been 10–15 km

thick in the northeastern Mount Stuart area. Isostatic considerations indicate that ≈20% of this thrust load would have been expressed as an increase in topography (2–3 km in the northeast Mount Stuart area). The increases in topography would have led directly to increases in erosion rates. Exhumation appears to have been primarily by erosion as extensional faults have not been recognized within the Cascade metamorphic core. Basins on both sides of the Cascade orogen show clear evidence for erosional exhumation at this time (Nanaimo basin to the west and Methow-Tyaughton basin to the east; McGroder, 1991). If the area remained well drained by rivers, then we would expect erosion to continue until the new topography and the underlying thrust load were removed. In this way, erosional exhumation would be expected to eventually return the batholith back to near its original configuration.

Paleomagnetic Data

Beck et al. (1981) published an extensive paleomagnetic data set for the southern part of the Mount Stuart batholith. They argued that the remanence was acquired during postmagmatic cooling following immediately after emplacement ("primary" remanence). Four lines of evidence lead us to conclude that Beck et al. (1981) did in fact report primary magnetization directions. (1) The representative stepwise alternating magnetic field (AF) demagnetization curves published by Beck et al. (1981) show a monotonic decay in remanent magnetization as would be expected for the removal of a single-component magnetization (cf. Irving et al., 1985). (2) The Mount Stuart batholith crystallized during the Cretaceous long-normal polarity interval (118–84 Ma). Beck et al.'s (1981) sites all had normal polarities, which is consistent with the measured remanence having been acquired soon after emplacement and crystallization of the batholith. (3) Beck et al. (1981) determined remanence directions for three sites in contact-metamorphosed peridotite exposed along the southwestern margin of the batholith and found that magnetic directions for the peridotite and the batholith do not differ significantly from one another. (4) Most of Beck et al.'s (1981) data are from the southern part of the batholith. As shown above, this part of the batholith was emplaced at the shallowest crustal levels and probably cooled quickly. Beck and Noson (1972) and Beck et al. (1981) were unable to measure a consistent remanence in the northern part of the batholith. This problem is consistent with the observation that the northern Mount Stuart area was overprinted by regional metamorphism. The metamorphism could have obscured or destroyed the primary remanence.

Lund et al. (1993, 1994) and Paterson et al. (1994) have started a new paleomagnetic study of the Mount Stuart batholith. This work is important because it provides a modern analysis of the Mount Stuart remanence using both AF and thermal demagnetization. These results have not yet been fully published and cannot be evaluated in detail, but some general conclusions seem warranted at this time. Lund et al. argued that the remanence is commonly carried by pyrrhotite. Fine-grained pyrrhotite would be expected to have a relatively high AF-demag coercivity but a relatively low blocking temperature of ≈300 °C (Geissman et al., 1982; Irving et al., 1985; Dekkers, 1988). We agree with Paterson et al. (1994) that pyrrhotite is a widespread phase in the batholith and that the mineral generally appears to be igneous in origin. Nonetheless, the possibility remains that some or even most of the remanence is carried by magnetite, because magnetite is much more magnetic than pyrrhotite. In addition, the magnetite carrier may be restricted to submicron-sized
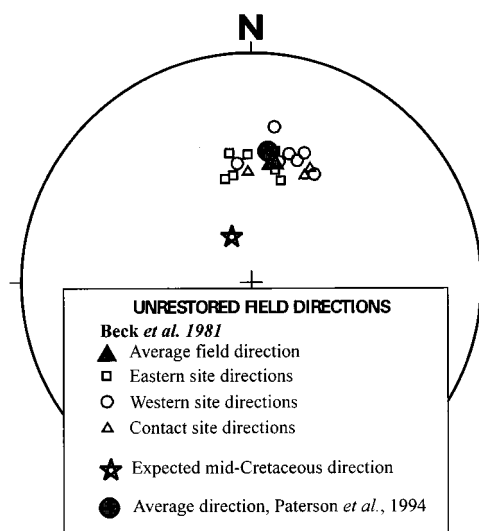
Figure 11. Paleomagnetic directions measured by Beck et al. (1981) and Paterson et al. (1994). Regional tilt corrections have not been applied to the data.

grains (e.g., Irving et al., 1985) and, therefore, would be extremely difficult to detect petrographically. The dominant carrier of the remanence will also vary with lithology, with more mafic rock types having a greater probability of containing a stable magnetite carrier. Thus we remain cautious about using the preliminary finding of the Lund et al. study to interpret the paleomagnetic data of Beck et al. (1981). For our discussion here, we conclude that the remanence is carried by some combination of very fine-grained magnetite and pyrrhotite. Furthermore, because both of these phases are probably of igneous origin, the remanence that they carry would be a thermal remanence acquired during cooling through the temperature range of ≈550–200 °C.

This range in magnetic blocking temperatures raises questions about when the magnetization in the southern part of the Mount Stuart batholith was acquired and if it may have been affected by tilting associated with regional-scale loading of the northern part of the batholith. The K/Ar closure temperatures for hornblende (550 °C) and biotite (300 °C) can be used to estimate the times at which stable magnetite and pyrrhotite carriers would have acquired a thermal remanent magnetization. The southern part of the batholith has generally yielded concordant K/Ar ages for hornblende and biotite pairs, with ages ranging from 93 to 82 Ma. These cooling ages fall almost entirely within the Cretaceous long-normal polarity interval (118–83 Ma), which would account for the normal polarity of the entire Beck et al. data set. Furthermore, we are forced to conclude that the Beck et al. directions would have been acquired while the northern part of the batholith was being loaded and exhumed. In this regard, it is interesting to note that the Beck et al. directions (Fig. 11) show no evidence of vertical smearing as would be expected if the magnetization was acquired while the body was tilting around a northwest-trending axis. From this relationship, we conclude that the southern part of the batholith was not involved in any significant manner with the loading and tilting so clearly recorded in the northern part of the batholith. Thus, the igneous paleohorizontal indicated by our AH barometry provides the reference frame needed to restore the magnetization direction of Beck et al. (1981). We note that the stepwise demagnetization experiments and associated com-
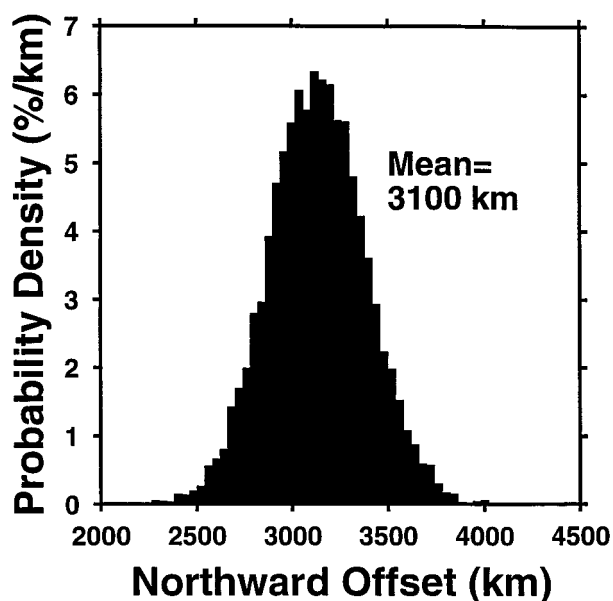
Figure 12. Histogram of replicate means of northward offset for the Mount Stuart batholith as determined by bootstrap resampling methods (Efron, 1982; Ague and Brandon, 1992). Vertical axis indicates probability of a given northward offset value. Distribution includes uncertainties associated with the best-fit paleohorizontal and mean virtual geomagnetic pole (VGP) direction for the Mount Stuart, and the mean VGP direction for coeval North American craton sites.

ponent analysis by Lund et al. should provide a rigorous test of our conclusion here, namely, that the southern batholith remained untilted during acquisition of its stable magnetization.

Paleomagnetic reference is needed to determine the relative northward offset of the Mount Stuart batholith with respect to the stable interior of North America. The North American cratonal reference frame for the middle Cretaceous is well established from widely separated sampling sites; virtual geomagnetic pole data used here are from Globerman and Irving (1988) and Van Fossen and Kent (1992).

Restoration of Paleomagnetic Data

The paleomagnetic data for the Mount Stuart batholith must be restored according to the best-fit paleohorizontal orientation before regional tectonic interpretations can be made. Standard Fisher statistics applied to the Beck et al. (1981) paleomagnetic data (uncorrected for tilt) yield a declination of 9.9°, an inclination of 45.6° and an α_{95} of 4.9°. Restoration of Beck et al.'s data using the best-fit paleohorizontal orientation yields declination and inclination estimates of 16.1° ± 8.0° and 49.4° ± 4.6°, respectively (±95% confidence). Using these restored data, we calculate a paleolatitude estimate of 30.3° ± 4.0° and rotation and northward offset estimates of 42° ± 11° (clockwise) and 3100 ± 600 km, respectively (±95% confidence) (Fig. 12). Thus we conclude that the batholith underwent tectonic tilting, clockwise rotation, *and* major northward offset. Beck et al. (1981) argued that northward motion resulted from interaction of the Mount Stuart region with the Kula or Farallon plates. These plates were moving northward relative to cratonal North America at rates on the order of ≈100 km/m.y. during Late

Cretaceous–early Tertiary time (cf. Engebretson et al., 1985, 1987) and thus could have facilitated northward transport.

TECTONIC IMPLICATIONS

The significance of our results are illustrated by Figure 13, which shows a Late Cretaceous reconstruction of western North America following Cowan (1994). This reconstruction attempts to account for both geologic and paleomagnetic constraints. Baja BC is now recognized to be restricted to the Insular belt and southern Coast plutonic complex (Cowan, 1994; Wynne et al., 1995). The eastern boundary of the block remains poorly resolved but is thought to coincide with the Pasayten fault in western Washington and southern British Columbia, and the tonalite sill of southeast Alaska (Cowan 1994; Garver and Brandon, 1994). The Mount Stuart results analyzed here and the Mount Tatlow results of Wynne et al. (1995) indicate some 3000 km of northward transport during the interval 85–55 Ma. Thus Baja BC would have originated at the latitude of present-day Baja California.

To the east of Baja BC lies another offset block, called here "Alta BC" (E. Irving, 1995, personal commun.). This block consists mainly of terranes of the Intermontane belt of Canada. It is bounded on its east side by the Tintina fault, which has ≈450 km of right-lateral displacement during the latest Cretaceous and early Tertiary (Price and Carmichael, 1986). The southern continuation of this structure has been obscured by Eocene extension in southern British Columbia and eastern Washington State (Price and Carmichael, 1986; Parrish et al., 1988). Paleomagnetic results from the middle Cretaceous Spences Bridge volcanics indicate a somewhat greater northward offset of ≈1100 km (Irving et al., 1995).

Baja Alaska (Packer and Stone, 1974) contains the Wrangellia and Southern Margin composite terranes and is bounded on its east and north sides by the Chatham Strait and Denali faults (Plafker and Berg, 1994). This block has yielded conflicting Late Cretaceous paleomagnetic data (Hillhouse and Coe, 1994). We emphasize here the MacColl results of Panuska (1985), which indicate some 4900 km of northward offset since the latest Cretaceous (Maastrichtian). The reconstruction in Figure 13 shows Baja Alaska as having originated along the west side of Baja BC. This result is consistent with the occurrence of the Wrangellia composite terrane in both blocks and with the evidence of truncation of the west side of Baja BC during the latest Cretaceous or early Tertiary (Brandon, 1989b). The reconstruction also shows an active subduction zone along the outboard side of Baja Alaska, as recorded by the Chugach terrane, which records subduction accretion during Late Cretaceous and early Tertiary time (Plafker et al., 1994). There is no comparable subduction complex preserved along the western side of Baja BC (Brandon, 1989a, 1989b), which is consistent with our reconstruction of a Baja Alaska flanking the west side of Baja BC.

Paleomagnetic data indicate that the Sierra Nevada batholith, Salinian block, and Peninsular Ranges batholith have been variably offset by some 500–1000 km since the middle Cretaceous (e.g., SN and PR summarized in Figure 13). These results indicate that Baja Alaska plus Baja BC would have originally lain outboard of the Peninsular Ranges batholith of Baja California. This arrangement is attributed to early Late Cretaceous collision of the Insular superterrane in a position south of the Sierra Nevada batholith (Brandon et al., 1988; Cowan, 1994).

It is interesting to note that magmatism in the Sierra Nevada, Salinian block, and Peninsular Ranges ceased at ca. 90–80 Ma
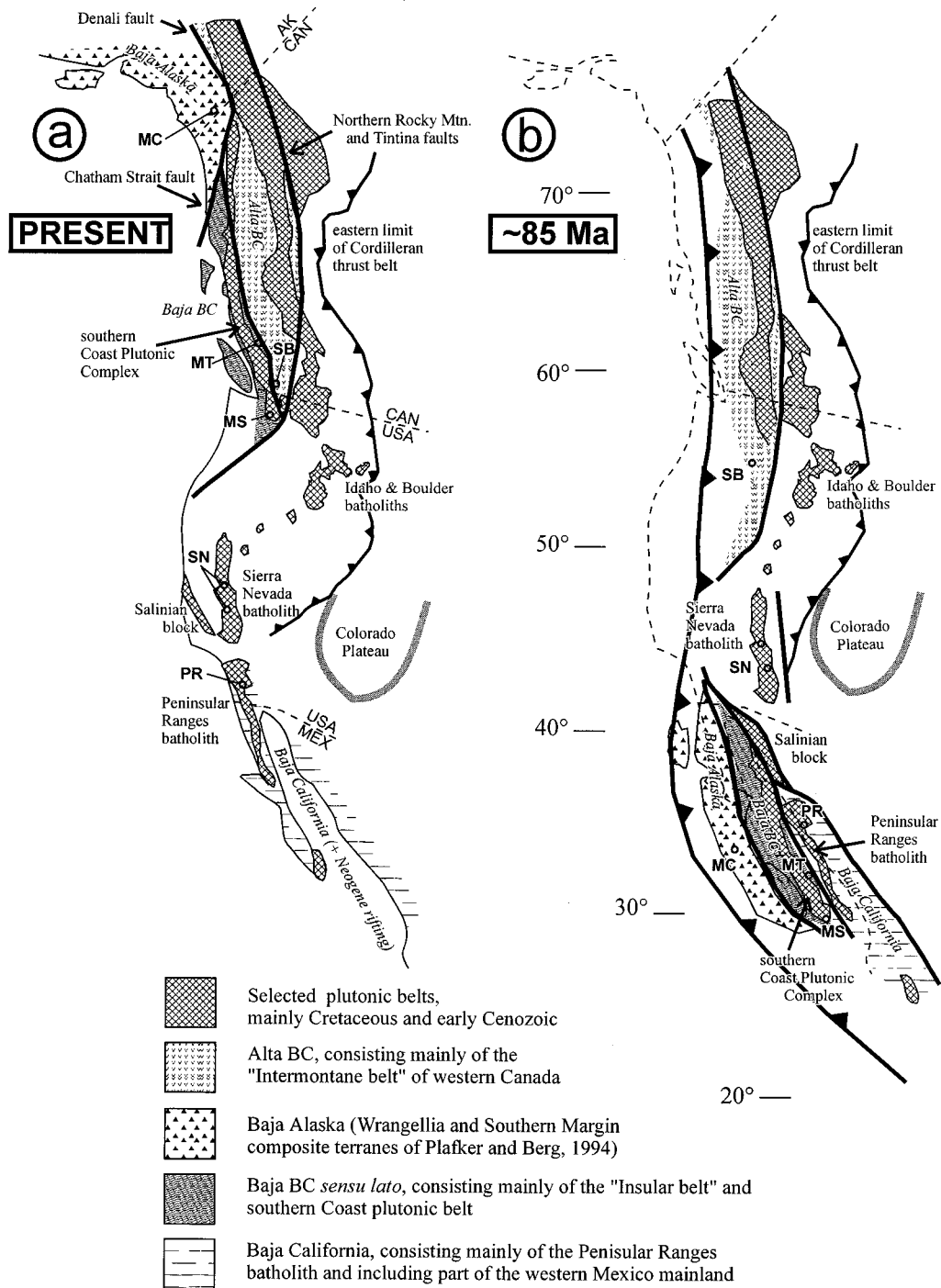
Figure 13. Late Cretaceous reconstruction of the western margin of the Cordillera following Cowan (1994). Tectonic elements have been selected to highlight the effects of latest Cretaceous–early Tertiary coastwise transport. A shows the present tectonic configuration, and B shows the configuration at 85 Ma, immediately following collision of the Insular superterrane (e.g., Monger et al., 1982; Brandon et al., 1988). The latitude scale and the dashed outline of the North American coast for part B are relative to the middle Cretaceous cratonal reference frame (Umhoefer, 1987). Abbreviations and predicted paleolatitudes for selected middle to Late Cretaceous paleomagnetic studies are MC = MacColl Ridge Formation, 32° ± 9° (Panuska, 1985); SB = Spences Bridge Group, 50.8° ± 5° (Irving et al., 1995); MT = Mount Tatlow area, 35.9° ± 3.5° (Wynne et al., 1995); MS = Mount Stuart batholith, 30.3° ± 4° (Beck et al. 1981; this paper); SN = Sierra Nevada batholith, 40° ± 7.6° (combined results, Frei, 1986); PR = Peninsular Ranges batholith, 34.8° ± 3.3° (Teissere and Beck, 1973; Hagstrum et al., 1985; Ague and Brandon, 1992).

(Cowan, 1992), immediately following the proposed collisional event. We propose that this transition does not mark a magmatic hiatus but rather a westward shift in magmatism to the Baja BC and Baja Alaska blocks, which contain numerous plutons of latest Cretaceous and early Tertiary age (Armstrong, 1988; Plafker and Berg, 1994). Our interpretation challenges the widely accepted idea of the Laramide magmatic lull, which is commonly attributed to shallow-slab subduction (Snyder et al., 1976; Dickinson and Snyder, 1978). In our interpretation, normal subduction with a moderately-dipping slab would have continued along the west side of Baja Alaska and Baja BC as these blocks migrated northward along the margin and outboard of an extinct Sierra Nevada arc and an inactive Franciscan subduction complex. Arc magmatism and subduction accretion would have been reinitiated during the Eocene after passage of Baja BC and Baja Alaska, which is consistent with the magmatic record of the western United States, which shows renewed volcanism along the "Laramide amagmatic corridor" during the Eocene (Dickinson and Snyder, 1978).

The final docking of Baja BC and Baja Alaska was completed by Eocene time (Irving and Wynne, 1990; Hillhouse and Coe, 1994). The entire northward motion and docking appears to have occurred entirely along conservative plate boundaries because there are no post–Early Cretaceous ophiolitic rocks or subduction complexes preserved along the inboard margins of these blocks. The identification of the specific strike-slip faults involved in this northward transport remains an active and controversial focus for current research along the western margin of the North American Cordillera.

ACKNOWLEDGMENTS

TABLE A1. SAMPLE LOCATIONS AND HORNBLENDE Al^{T}*

Sample	X (km)	Y (km)	Z_E† (km)	Al^T
MS-002	7.87	2.37	1.74	0.87
MS-003	7.73	2.63	1.84	0.93
MS-017	3.18	6.08	1.65	1.04
MS-028	9.70	−13.49	1.54	0.86
MS-037	12.11	−13.06	1.53	0.82
MS-047	11.91	−14.42	1.89	0.85
MS-053	22.05	−8.84	0.67	0.91
MS-086	16.42	−15.14	2.11	0.88
MS-094	13.84	−15.21	2.38	0.84
MS-101B	24.26	−3.30	0.37	0.94
MS-103	24.35	−3.24	0.37	0.99
MS-110B	24.23	−3.26	0.37	0.88
MS-112	−1.88	0.19	1.18	1.18
MS-120	−2.00	1.52	1.70	0.94
MS-131	−3.77	−2.50	1.23	1.01
MS-134	−4.63	−2.71	1.59	1.08
MS-140	−4.94	−2.39	1.55	0.93
MS-147	−14.29	9.41	0.77	1.12
MS-149	−14.26	9.14	0.82	1.14
MS-151	−13.98	8.41	0.88	1.20
MS-152B	−13.95	8.30	0.91	1.12
MS-156	−13.36	6.12	0.93	1.15
MS-171	−13.07	15.34	1.04	1.25
MS-179	−15.21	11.03	0.50	1.35
MS-194	−9.79	11.17	0.78	1.14
MS-199	−9.28	11.16	0.85	1.22
MS-206	−9.28	13.79	1.05	1.17
MS-207	−9.20	13.95	1.06	1.17
MS-210	−9.00	14.32	1.07	N.D.§
MS-216	−6.46	12.64	1.50	1.12
MS-220	−6.35	12.86	1.54	1.09
MS-224	−5.33	11.75	1.39	1.16
MS-239	−3.22	18.25	0.99	1.05
MS-246	−2.16	18.62	0.96	1.06
MS-252	2.10	17.23	0.84	1.32
MS-253	1.52	16.94	0.85	1.26
MS-258	−0.56	17.44	0.96	1.17
MS-261	−3.02	22.15	1.26	1.10
MS-262	−3.12	22.03	1.28	1.33
MS-263	−3.27	21.90	1.29	1.03
MS-267	−5.77	20.64	1.24	0.99
MS-275	−15.62	23.57	0.69	1.61
MS-280	−14.09	23.24	0.70	1.11
MS-291	−8.82	24.15	1.59	1.16
MS-300	−10.52	25.17	1.55	1.22
MS-305	13.97	−2.50	0.74	N.D.§
WP-454#	6.21	−15.58	2.13	0.86
WP-545#	6.27	−6.37	1.87	1.13
WP-549#	5.60	−8.34	2.07	0.80

Note: X = 0 km, Y = 0 km at long 239°E, lat 47.617°N, respectively.

*Total Al in hornblende (formula units; 23 oxygen atoms).

†Sample elevation.

§N.D. = no data.

#Sample collected by Pongsapich (1974).

TABLE A2. HORNBLENDE ANALYSES

Sample	SiO_2	TiO_2	Al_2O_3	FeO	MgO	MnO	CaO	Na_2O	K_2O	F	Cl	Total
MS-002	50.31	0.51	5.07	14.29	13.67	0.45	11.99	0.64	0.42	0.01	0.01	97.37
MS-003	49.27	0.54	5.39	16.27	12.57	0.56	11.86	0.79	0.50	0.08	0.01	97.84
MS-017	49.32	0.67	6.01	15.75	12.25	0.49	11.93	0.74	0.54	0.05	0.03	97.78
MS-028	50.58	0.50	5.11	14.23	14.49	0.39	12.22	0.70	0.38	0.05	0.03	98.68
MS-037	51.27	0.42	4.91	13.56	15.15	0.34	12.25	0.66	0.32	0.02	0.04	98.94
MS-047	50.10	0.50	5.00	14.91	14.23	0.40	12.01	0.80	0.42	0.02	0.06	98.45
MS-053	50.83	0.38	5.43	13.19	14.97	0.31	12.40	0.65	0.37	0.05	0.04	98.62
MS-086	50.32	0.49	5.21	14.60	14.42	0.38	12.18	0.78	0.43	0.03	0.04	98.88
MS-094	50.53	0.52	4.98	14.47	14.47	0.37	12.07	0.71	0.40	0.04	0.05	98.61
MS-101B	51.06	0.47	5.65	12.63	15.36	0.30	12.18	0.71	0.43	0.02	0.05	98.86
MS-103	50.49	0.55	5.89	12.51	15.21	0.27	12.09	0.79	0.49	0.04	0.09	98.42
MS-110B	51.58	0.39	5.29	12.00	15.95	0.31	12.21	0.73	0.38	0.03	0.04	98.91
MS-112	48.06	0.56	6.86	14.74	13.26	0.30	11.91	0.81	0.49	0.04	0.02	97.05
MS-120	49.56	0.56	5.45	14.31	13.69	0.40	11.98	0.72	0.45	0.03	0.02	97.17
MS-131	48.50	0.47	5.85	15.04	13.45	0.43	11.84	0.86	0.43	0.04	0.02	96.93
MS-134	49.38	0.61	6.41	14.71	13.83	0.44	11.52	0.90	0.54	0.04	0.03	98.41
MS-140	49.92	0.42	5.47	14.65	14.16	0.44	11.80	0.81	0.41	0.03	0.02	98.13
MS-147	49.10	0.47	6.59	14.37	13.98	0.29	11.82	0.91	0.51	0.05	0.02	98.11
MS-149	48.22	0.76	6.66	16.47	12.64	0.27	11.60	1.12	0.70	0.12	0.06	98.62
MS-151	47.65	0.79	6.98	16.77	12.20	0.23	11.69	1.10	0.72	0.14	0.07	98.34
MS-152B	48.41	0.71	6.48	16.43	12.45	0.23	11.73	1.01	0.68	0.16	0.07	98.36
MS-156	48.49	0.72	6.73	15.61	12.96	0.24	11.86	0.92	0.65	0.09	0.10	98.37
MS-171	48.70	0.39	7.30	14.82	13.14	0.28	11.80	0.85	0.23	0.02	0.02	97.55
MS-179	46.24	0.56	7.66	17.10	11.38	0.25	11.94	1.14	0.75	0.14	0.09	97.25
MS-194	48.92	0.46	6.66	15.01	13.09	0.23	11.66	0.73	0.24	0.02	0.03	97.05
MS-199	48.40	0.44	7.06	14.88	12.97	0.30	11.74	0.83	0.30	0.03	0.03	96.98
MS-206	48.51	0.36	6.77	16.68	11.62	0.51	12.06	0.67	0.51	0.00	0.01	97.70
MS-207	48.28	0.41	6.74	16.35	11.93	0.50	12.04	0.68	0.55	0.06	0.01	97.55
MS-216	48.34	0.36	6.43	16.70	11.56	0.53	12.01	0.66	0.47	0.05	0.02	97.13
MS-220	49.08	0.33	6.28	15.96	11.78	0.52	11.96	0.65	0.47	0.07	0.01	97.11
MS-224	48.05	0.34	6.65	17.09	11.37	0.51	12.04	0.70	0.51	0.07	0.02	97.35
MS-239	49.65	0.21	6.11	14.29	13.49	0.47	12.17	0.68	0.47	0.04	0.01	97.59
MS-246	50.19	0.29	6.21	13.37	14.04	0.27	12.24	0.61	0.43	0.04	0.02	97.71
MS-252	49.62	0.35	7.82	13.42	13.42	0.27	12.14	0.76	0.46	0.02	0.03	98.31
MS-253	48.73	0.35	7.33	13.80	13.27	0.37	12.18	0.73	0.57	0.03	0.01	97.37
MS-258	49.59	0.31	6.85	13.32	13.94	0.38	12.15	0.66	0.43	0.03	0.01	97.67
MS-261	49.98	0.20	6.41	13.94	13.39	0.32	12.37	0.71	0.45	0.05	0.00	97.82
MS-262	48.48	0.34	7.70	14.24	12.47	0.34	12.21	0.82	0.62	0.07	0.00	97.29
MS-263	50.12	0.26	6.00	12.45	14.32	0.23	12.22	0.67	0.37	0.04	0.00	97.68
MS-267	49.87	0.37	5.78	14.26	13.47	0.54	11.88	0.68	0.37	0.05	0.01	97.28
MS-275	44.87	0.60	9.08	17.51	10.48	0.49	11.83	0.87	0.96	0.07	0.04	96.80
MS-280	49.56	0.47	6.46	14.33	13.14	0.44	12.05	0.67	0.56	0.07	0.02	97.77
MS-291	48.91	0.42	6.78	14.06	13.35	0.46	12.09	0.69	0.52	0.03	0.01	97.32
MS-300	48.29	0.48	7.04	14.97	12.64	0.50	11.95	0.77	0.63	0.04	0.01	97.32
WP-454	50.57	0.58	5.13	13.52	15.20	0.25	12.04	0.72	0.40	0.03	0.07	98.51
WP-545	48.47	0.72	6.59	14.44	13.66	0.35	12.28	0.82	0.55	0.02	0.09	97.99
WP-549	50.75	0.73	4.70	13.85	14.32	0.35	12.19	0.57	0.38	0.02	0.04	97.90

Notes: All Fe as FeO. All measurements in wt%.

TABLE A3. BIOTITE, MUSCOVITE, GARNET, PLAGIOCLASE, AND K-FELDSPAR ANALYSES

Sample	SiO_2	TiO_2	Al_2O_3	FeO	MgO	MnO	CaO	BaO	Na_2O	K_2O	F	Cl	Total
Biotite													
MS-210	35.50	1.84	19.37	20.53	8.38	0.60	N.D.	0.19	0.11	9.35	0.11	0.02	95.89
MS-305	36.26	3.25	19.67	17.80	9.43	0.07	N.D.	0.29	0.15	9.59	0.11	0.05	96.67
Muscovite													
MS-210	46.86	0.41	35.74	1.70	0.98	0.03	N.D.	0.34	0.37	9.30	0.02	0.00	95.75
Garnet													
MS-210	36.32	0.02	21.15	24.01	1.53	14.57	1.77	N.D.	N.D.	N.D.	N.D.	N.D.	99.37
MS-305	37.52	0.04	21.74	32.28	4.66	3.05	1.65	N.D.	N.D.	N.D.	N.D.	N.D.	100.96
Plagioclase													
MS-003	62.64	N.D.	23.48	0.01	N.D.	N.D.	4.90	N.D.	8.69	0.13	N.D.	N.D.	99.85
MS-028	62.87	N.D.	23.50	0.16	N.D.	N.D.	4.88	N.D.	8.64	0.24	N.D.	N.D.	100.31
MS-103	60.82	N.D.	24.59	0.15	N.D.	N.D.	6.23	N.D.	7.95	0.13	N.D.	N.D.	99.88
MS-112	61.09	N.D.	24.28	0.15	N.D.	N.D.	5.90	N.D.	8.19	0.21	N.D.	N.D.	99.82
MS-131	63.69	N.D.	22.66	0.18	N.D.	N.D.	3.98	N.D.	9.19	0.19	N.D.	N.D.	99.88
MS-171	60.56	N.D.	24.94	0.04	N.D.	N.D.	6.53	N.D.	7.89	0.08	N.D.	N.D.	100.03
MS-206	59.93	N.D.	25.30	0.05	N.D.	N.D.	7.05	N.D.	7.59	0.13	N.D.	N.D.	100.05
MS-275	60.96	N.D.	24.73	0.22	N.D.	N.D.	6.17	N.D.	7.95	0.17	N.D.	N.D.	100.20
MS-210	61.53	N.D.	24.07	0.03	N.D.	N.D.	4.66	N.D.	8.93	0.20	N.D.	N.D.	99.42
MS-305	55.51	N.D.	28.73	0.10	N.D.	N.D.	9.68	N.D.	6.02	0.20	N.D.	N.D.	100.24
WP-454	62.99	N.D.	23.84	N.D.	N.D.	N.D.	4.93	N.D.	8.40	0.29	N.D.	N.D.	100.45
WP-545	59.47	N.D.	24.95	N.D.	N.D.	N.D.	6.62	N.D.	7.76	0.35	N.D.	N.D.	99.15
K-feldspar													
MS-210	62.65	N.D.	19.63	0.01	N.D.	N.D.	0.00	1.58	0.79	14.99	N.D.	N.D.	99.65
MS-305	62.48	N.D.	19.56	0.05	N.D.	N.D.	0.00	1.70	1.27	14.29	N.D.	N.D.	99.35

Notes: All Fe as FeO. All measurements in wt%. N.D. = not determined. Mineral abbreviations from Kretz (1983). Plagioclase analyses for WP-454 and WP-545 are from Pongsapich (1974).

APPENDIX

The Appendix presents information on sample locations and hornblende Al^T (Table A1), hornblende analyses (Table A2), and analyses of biotite, muscovite, garnet, plagioclase, and potassium feldspar (Table A3).

REFERENCES CITED

Ague, J. J., 1994, Mass transfer during Barrovian metamorphism of pelites, south-central Connecticut, I: Evidence for composition and volume change: American Journal of Science, v. 294, p. 989–1057.

Ague, J. J., and Brandon, M. T., 1992, Tilt and northward offset of Cordilleran batholiths resolved using igneous barometry: Nature, v. 360, p. 146–149.

Ague, J. J., and Brimhall, G. H., 1988, Magmatic arc asymmetry and distribution of anomalous plutonic belts in the batholiths of California: Effects of assimilation, crustal thickness, and depth of crystallization: Geological Society of America Bulletin, v. 100, p. 912–927.

Anderson, J. L., and Smith, D. R., 1993, Success and failure of the Al-in-hornblende barometer: Geological Society of America Abstracts with Programs, v. 25, p. A41.

Anderson, J. L., and Smith, D. R., 1995, The effects of temperature and oxygen fugacity on the Al-in-hornblende barometer: American Mineralogist, v. 80, p. 549–559.

Armstrong, R. L., 1988, Mesozoic and early Cenozoic magmatic evolution of the Canadian Cordillera: Geological Society of America Special Paper 218, p. 55–91.

Beck, M. E., Jr., 1989, Paleomagnetism of continental north America: Implications for displacement of crustal blocks within the western Cordillera, Baja California to British Columbia, *in* Pakiser, L. C., and Mooney, W. D., eds., Geophysical framework of the continental United States: Geological Society of America Memoir 172, p. 471–492.

Beck, M. E., Jr., 1991, Some thermal and paleomagnetic consequences of tilting a batholith: Tectonics, v. 11, p. 297–302.

Beck, M. E., and Noson, L., 1972, Anomalous paleolatitude in Cretaceous granitic rocks: Nature, v. 235, p. 11–13.

Beck, M. E., Burmester, R. F., and Schoonover, R., 1981, Paleomagnetism and tectonics of the Cretaceous Mt. Stuart batholith of Washington: Translation or tilt?: Earth and Planetary Science Letters, v. 56, p. 336–342.

Berman, R. G., 1988, Internally-consistent thermodynamic data for minerals in the system Na_2O-K_2O-CaO-MgO-FeO-Fe_2O_3-Al_2O_3-SiO_2-TiO_2-H_2O-CO_2: Journal of Petrology, v. 29, p. 445–522.

Berman, R. G., 1991, Thermobarometry using multi-equilibrium calculations: A new technique, with petrological applications: Canadian Mineralogist, v. 29, p. 833–855.

Blundy, J. D., and Holland, T. J. B., 1990, Calcic amphibole equilibria and a new amphibole-plagioclase geothermometer: Contributions to Mineralogy and Petrology, v. 104, p. 208–224.

Blundy, J. D., and Holland, T. J. B., 1992a, "Calcic amphibole equilibria and a new amphibole-plagioclase geothermometer": Reply to the comments of Hammarstrom and Zen and Rutherford and Johnson: Contributions to Mineralogy and Petrology, v. 104, p. 269–272.

Blundy, J. D., and Holland, T. J. B., 1992b, "Calcic amphibole equilibria and a new amphibole-plagioclase geothermometer": Reply: Contributions to Mineralogy and Petrology, v. 104, p. 278–282.

Brandon, M. T., 1989a, Deformational styles in a sequence of olistostromal melanges, Pacific Rim Complex, western Vancouver Island, Canada: Geological Society of America Bulletin, v. 101, p. 1520–1542.

Brandon, M. T., 1989b, Origin of igneous rocks associated with melanges of the Pacific Rim Complex, western Vancouver Island, Canada: Tectonics, v. 8, p. 1115–1136.

Brandon, M. T., Cowan, D. S., and Vance, J. A., 1988, The Late Cretaceous San Juan thrust system, San Juan Islands, Washington: A case history of terrane accretion in the western Cordillera: Geological Society of America Special Paper 221, 81 p.

Brown, E. H., and Burmester, R. F., 1991, Metamorphic evidence for tilt of the Spuzzum pluton: Diminished basis for the "Baja British Columbia" concept: Tectonics, v. 10, p. 978–985.

Brown, E. H., and Walker, N. W., 1993, A magma-loading model for Barrovian metamorphism in the southeast coast plutonic complex, British Columbia and Washington: Geological Society of America Bulletin, v. 105, p. 479–500.

Butler, R. F., Gehrels, G. E., McClelland, W. C., May, S. R., and Klepacki, D., 1989, Discordant paleomagnetic poles from the Canadian Coast Plutonic Complex: Regional tilt rather than large-scale displacement?: Geology, v. 17, p. 691–694.

Cosca, M. A., Essene, E. J., and Bowman, J. R., 1991, Complete chemical analyses of metamorphic hornblendes: Implications for normalizations, calculated H_2O activities and thermobarometry: Contributions to Mineralogy and Petrology, v. 108, p. 472–484.

Cowan, D. S., 1994, Alternative hypotheses for the mid-Cretaceous paleogeography of the western Cordillera: GSA Today, v. 4, p. 181–186.

Cowan, D. S., and Bruhn, R. L., 1992, Late Jurassic to early Late Cretaceous geology of the U.S. Cordillera, *in* Burchfiel, B. C., Lipman, P. W., and Zoback, M. L., eds., The Cordilleran orogen: Conterminous U.S.: Boulder, Colorado, Geological Society of America, Geology of North America, v. G-3: p. 169–203.

Dekkers, M., 1988, Some rock magnetic parameters for natural goethite, pyrrhotite, and fine-grained hematite: Geologica Ultraiectina, v. 51, p. 231.

Dickinson, W., and Snyder, W., 1978, Plate tectonics of the Laramide orogeny: Geological Society of America Memoir 151, p. 355–366.

Efron, B., 1982, The jackknife, the bootstrap and other resampling plans: CBMS-NSF Regional Conference Series in Applied Mathematics, SIAM, v. 38, 92 p.

Efron, B., and Tibshirani, R. J., 1993, An introduction to the bootstrap: New York, Chapman and Hall, 436 p.

Engebretson, D. C., Gordon, R. G., and Cox, A., 1985, Relative motions between oceanic and continental plates in the Pacific basin: Geological Society of America Special Paper 206, 59 p.

Engebretson, D. C., Cox, A., and Debiche, M., 1987, Reconstructions, plate interactions, and trajectories of oceanic and continental plates in the Pacific Basin, *in* Monger, J. W. H., and Francheteau, J., eds., Circum-Pacific orogenic belts and evolution of the Pacific Ocean basin: Geodynamics Series, v. 18, p. 19–27.

Erikson, E. H., Jr., 1977, Petrology and petrogenesis of the Mt. Stuart batholith—Plutonic equivalent of the high alumina basalt association?: Contributions to Mineralogy and Petrology, v. 60, p. 183–207.

Erikson, E. H., Jr., and Williams, A. E., 1976, Implications of apatite fission track ages in the Mount Stuart batholith, Cascade Mountains, Washington: Geological Society of America Abstracts with Programs, v. 8, p. 372.

Evans, B. W., and Berti, J. W., 1986, Revised metamorphic history for the Chiwaukum schist, North Cascades, Washington: Geology, v. 14, p. 695–698.

Evans, D. A., Lasaga, A. C., Ague, J. J., and Brandon, M. T., 1993, Geospeedometry and the met-

amorphic history of the Late Cretaceous Chiwaukum Schist, west central Washington State: Geological Society of America Abstracts with Programs, v. 25, no. 5, p. 36.

Fisher, R. A., 1953, Dispersion on a sphere: Proceedings of the Royal Society of London, Ser. A, v. 217, p. 295–305.

Freer, R., 1981, Diffusion in silicate melts and glasses: A data digest and guide to the literature: Contributions to Mineralogy and Petrology, v. 76, p. 440–454.

Frei, L., 1986, Additional paleomagnetic results from the Sierra Nevada: Further constraints on Basin and Range extension and northward displacement in the western United States: Geological Society of America Bulletin, v. 97, p. 840–849.

Frizzell, V. A., Jr., Tabor, R. W., Booth, D. B., Ort, K. M., and Waitt, R. B., Jr., 1984, Preliminary geologic map of the Snoqualmie Pass 1:100,000 quadrangle, Washington: U.S. Geological Survey Open File Report 84-693.

Frost, B. R., 1975, Contact metamorphism of serpentinite, chloritic blackwall and rodingite at Paddy-Go-Easy Pass, central Cascades, Washington: Journal of Petrology, v. 16, p. 272–313.

Fuhrman, M. L., and Lindsley, D. H., 1988, Ternary-feldspar modeling and thermometry: American Mineralogist, v. 73, p. 201–215.

Garver, J. I., and Brandon, M. T., 1994, Fission-track ages of detrital zircons from Cretaceous strata, southern British Columbia; Implications for the Baja BC hypothesis: Tectonics, v. 13, p. 401–420.

Geissman, J., Strangway, D., and Tasillo-Hirt, A. M., 1982, Paleomagnetism and structural history of the Ghost Range intrusive complex, central Abitibi Belt, Ontario; Further evidence of the late Archean geomagnetic field of North America: Canadian Journal of Earth Sciences, v. 19, p. 2085–2099.

Globerman, B. R., and Irving, E., 1988, Mid-Cretaceous paleomagnetic reference field for North America: Restudy of 100 Ma intrusive rocks from Arkansas: Journal of Geophysical Research, v. 93, p. 11,721–11,733.

Grow, J. A., and Bowin, C. O., 1975, Evidence for high-density crust and mantle beneath the Chile trench due to the descending lithosphere: Journal of Geophysical Research, v. 80, p. 1449–1458.

Hagstrum, J. T., McWilliams, M., Howell, D. G., and Grommé, S., 1985, Mesozoic paleomagnetism and northward translation of the Baja California Peninsula: Geological Society of America Bulletin, v. 96, p. 1077–1090.

Hammarstrom, J. M., and Zen, E-an, 1986, Aluminum in hornblende: An empirical igneous geobarometer: American Mineralogist, v. 71, p. 1297–1313.

Hammarstrom, J. M., and Zen, E-an, 1992, Discussion of Blundy and Holland's (1990) "Calcic amphibole equilibria and a new amphibole-plagioclase thermometer": Contributions to Mineralogy and Petrology, v. 111, p. 264–268.

Haugerud, R. A., Van Der Heyden, P., Tabor, R. W., Stacey, J. S., and Zartman, R. E., 1991, Late Cretaceous and early Tertiary plutonism and deformation in the Skagit Gneiss Complex, North Cascade Range, Washington and British Columbia: Geological Society of America Bulletin, v. 103, p. 1297–1307.

Hillhouse, J., and Coe, R., 1994, Paleomagnetic data from Alaska, in Plafker, G., and Berg, H., eds., The geology of Alaska: Boulder, Colorado, Geological Society of America, Geology of North America, G-1, p. 797–812.

Holland, T., and Blundy, J., 1994, Non-ideal interactions in calcic amphiboles and their bearing on amphibole-plagioclase thermometry: Contributions to Mineralogy and Petrology, v. 116, p. 433–447.

Hollister, L. S., Grissom, G. C., Peters, E. K., Stowell, H. H., and Sisson, V. B., 1987, Confirmation of the empirical correlation of Al in hornblende with pressure of solidification of calc-alkaline plutons: American Mineralogist, v. 72, p. 231–239.

Irving, E., and Brandon, M. T., 1990, Paleomagnetism of the Flores volcanics, Vancouver Island, in place by Eocene time: Canadian Journal of Earth Sciences, v. 27, p. 811–817.

Irving, E. and Wynne, P. J., 1990, Paleomagnetic evidence bearing on the evolution of the Canadian Cordillera: Philosophical Transactions of the Royal Society of London, v. A 331, p. 487–509.

Irving, E., Woodsworth, G. J., Wynne, P. J., and Morrison, A., 1985, Paleomagnetic evidence for displacement from the south of the Coast Plutonic Complex, British Columbia: Canadian Journal of Earth Sciences, v. 22, p. 584–598.

Irving, E., Thorkelson, D. J., Wheadon, P. M., and Enkin, R. J., 1995, Paleomagnetism of the Spences Bridge Group and northward displacement of the Intermontane Belt, British Columbia: A second look: Journal of Geophysical Research, v. 100, p. 6057–6071.

Ishihara, S., 1977, The magnetite-series and ilmenite-series granitic rocks: Mining Geology, v. 27, p. 293–305.

Johnson, M. C., and Rutherford, M. J., 1989, Experimental calibration of the aluminum-in-hornblende geobarometer with application to Long Valley caldera (California) volcanic rocks: Geology, v. 17, p. 837–841.

Kelemen, P. B., and Ghiorso, M. S., 1986, Assimilation of peridotite in zoned calc-alkaline plutonic complexes: Evidence from the Big Jim Complex, Washington Cascades: Contributions to Mineralogy and Petrology, v. 94, p. 12–28.

Kretz, R., 1983, Symbols for rock-forming minerals: American Mineralogist, v. 68 p. 277–279.

Lund, S. P., Paterson, S., and Anderson, L., 1993, Paleomagnetism and rock magnetism of the Mt. Stuart Batholith: Reassessment of discordant paleomagnetic results [abs.]: EOS (Transactions, American Geophysical Union), v. 74, p. 206.

Lund, S. P., Paterson, S., and Anderson, L., 1994, Paleomagnetism and rock magnetism of the Mt. Stuart Batholith: Reassessment of discordant paleomagnetic results: Geological Society of America Abstracts with Programs, v. 26, p. A460.

McGroder, M. F., 1991, Reconciliation of two-sided thrusting, burial metamorphism, and diachronous uplift in the Cascades of Washington and British Columbia: Geological Society of America Bulletin, v. 103, p. 189–209.

McMullin, D. W. A., Berman, R. G., and Greenwood, H. J., 1991, Calibration of the SGAM thermobarometer for pelitic rocks using data from phase-equilibrium experiments and natural assemblages: Canadian Mineralogist, v. 29, p. 889–908.

Mengel, F. C., and Rivers, T., 1991, Decompression reactions and P-T conditions in high grade rocks, northern Labrador: P-T-t paths from individual samples and implications for early Proterozoic tectonic evolution: Journal of Petrology, v. 32, p. 139–167.

Merrill, R. B., Robertson, J. K., and Wyllie, P. J., 1970, Melting reactions in the system NaAlSi₃O₈-SiO₂-H₂O to 20 kilobars compared with results for other feldspar-quartz-H₂O and rock-H₂O systems: Journal of Geology, v. 78, p. 558–569.

Miller, R. B., 1985, The ophiolitic Ingalls Complex, North Cascades, Washington: Geological Society of America Bulletin, v. 96, p. 27–42.

Miller, R. B., and Paterson, S. R., 1992, Tectonic implications of syn- and post-emplacement deformation of the Mount Stuart batholith for mid-Cretaceous orogenesis in the North Cascades: Canadian Journal of Earth Sciences, v. 29, p. 479–485.

Miller, R. B., and Paterson, S. R., 1994, The transition from magmatic to high-temperature solid-state deformation: Implications from the Mount Stuart batholith, Washington: Journal of Structural Geology, v. 16, p. 853–865.

Miller, R. B., Johnson, S. Y., and McDougall, J. W., 1990, Discordant paleomagnetic poles from the Canadian Coast Plutonic Complex: Regional tilt rather than large displacement?: Comment: Geology, v. 18, p. 1164–1165.

Oldow, J. S., Bally, A. W., Avé Lallemant, H. G., and Leeman, W. P., 1989, Phanerozoic evolution of the North American Cordillera; United States and Canada, in Bally, A. W., and Palmer, A. R., eds., The geology of North America—An overview: Boulder, Colorado, Geological Society of America, Geology of North America, v. A, p. 139–232.

Packer, D. R., and Stone, D. B., 1974, Paleomagnetism of Jurassic rocks from southern Alaska and the tectonic implications: Canadian Journal of Earth Sciences, v. 11, p. 976–997.

Panuska, B., 1985, Paleomagnetic evidence for a post-Cretaceous accretion of Wrangellia: Geology, v. 13, p. 880–883.

Parrish, R. R., Carr, S. D., and Parkinson, D. L., 1988, Eocene extensional tectonics and geochronology of the southern Omineca belt, British Columbia and Washington: Tectonics, v. 7, p. 181–212.

Paterson, S. R., Miller, R. B., Anderson, J. L., Lund, S., Bendixen, J., Taylor, N., and Fink, T., 1994, Emplacement and evolution of the Mt. Stuart batholith, in Swanson, D. A., and Haugerud, R. A., eds., Guides to field trips, 1994: Seattle, Washington, Geological Society of America Annual Meeting, Chapter 2F.

Plafker, G., and Berg, H., 1994, Overview of the geology and tectonic evolution of Alaska, in Plafker, G., Berg, H., eds., The Geology of Alaska: Boulder, Colorado, Geological Society of America, Geology of North America, v. G-1, p. 989–1021.

Plafker, G., Moore, J., and Winkler, G., 1994, Geology of the southern Alaska margin, in Plafker, G., and Berg, H., eds., The geology of Alaska: Boulder, Colorado, Geological Society of America, Geology of North America, v. G-1, p. 389–449.

Plummer, C. N., 1980, Dynamothermal contact metamorphism superposed on regional metamorphism in the pelitic rocks of the Chiwaukum Mountains area, Washington Cascades: Summary: Geological Society of America Bulletin, v. 91, pt. I, p. 386–388.

Poli, S., and Schmidt, M. W., 1992, Calcic amphibole equilibria and a new amphibole-plagioclase thermometer: Comment: Contributions to Mineralogy and Petrology, v. 111, p. 273–282.

Pongsapich, W., 1974, Geology of the eastern part of the Mt. Stuart batholith, central Cascades [Ph.D. thesis]: Seattle, University of Washington, 170 p.

Price, R. A., and Carmichael, D. M., 1986, Geometric test for Late Cretaceous–Paleocene intracontinental transform faulting in the Canadian Cordillera: Geology, v. 14, p. 468–471.

Rutherford, M. J., and Johnson, M. C., 1992, Calcic amphibole equilibria and a new amphibole-plagioclase thermometer: Comment: Contributions to Mineralogy and Petrology, v. 111, p. 266–268.

Schmidt, M. W., 1992, Amphibole composition in tonalite as a function of pressure: An experimental calibration of the Al-in-hornblende barometer: Contributions to Mineralogy and Petrology, v. 110, p. 304–310.

Schmidt, M. W., 1993, Phase relations and compositions in tonalite as a function of pressure: An experimental study at 650°C: American Journal of Science, v. 293, p. 1011–1060.

Snyder, W., Dickinson, W., and Silberman, M., 1976, Tectonic implications of space-time patterns of Cenozoic volcanism in western United States: Earth and Planetary Science Letters, v. 32, p. 91–106.

Spear, F. S., 1981, An experimental study of hornblende stability and compositional variability in amphibolites: American Journal of Science, v. 281, p. 697–734.

Tabor, R. W., Waitt, R. B., Jr., Frizzell, V. A., Jr., Swanson, D. A., Byerly, G. R., and Bentley, R. D., 1982, Geologic map of the Wenatchee quadrangle, Washington: U.S. Geological Survey Miscellaneous Investigations Map MI-1311, scale 1:100 000.

Tabor, R. W., Frizzell, V. A., Jr., Whetten, J. T., Waitt, R. B., Swanson, D. A., Byerly, G. R., Booth, D. B., Hetherington, M. J., and Zartman, R. E., 1987, Geologic map of the Chelan 30-minute by 60-minute quadrangle, Washington: U.S. Geological Survey Miscellaneous Investigations Series Map I-1661, scale 1:100 000, 1 sheet, 33 p.

Tabor, R. W., Frizzell, V. A., Jr., Booth, D. B., Waitt, R. B., Whetten, J. T., and Zartman, R. E., 1993, Geologic map of the Skykomish River 30- by 60-minute quadrangle, Washington: U.S. Geological Survey Miscellaneous Investigations Series Map I-1963.

Tauxe, L., Kylstra, N., and Constable, C., 1991, Bootstrap statistics for paleomagnetic data: Journal of Geophysical Research, v. 96, p. 11,723–11,740.

Taylor, J. R., 1982, An introduction to error analysis: Mill Valley, University Science Books, Oxford University Press, 270 p.

Teissere, R. F., and Beck, M. E., Jr., 1973, Divergent paleomagnetic pole position for the southern California batholith: Earth and Planetary Science Letters, v. 18, p. 296–300.

Tichelaar, B. W., and Ruff, L. J., 1989, How good are our best models?: EOS (Transactions of the American Geophysical Union), v. 70, p. 595–606.

Umhoefer, P. J., 1987, Northward translation of "Baja British Columbia" along the Late Cretaceous to Paleocene margin of western North America: Tectonics, v. 6, p. 377–394.

Umhoefer, P. J., and Magloughlin, J. F., 1990, Discordant paleomagnetic poles from the Canadian Coast Plutonic Complex: Regional tilt rather than large displacement?: Comment: Geology, v. 18, p. 800–801.

Umhoefer, P. J., Dragovich, J., Cary, J., and Engebretson, D. C., 1989, Refinements of the "Baja British Columbia" plate-tectonic model for northward translation along the margin of western North America, in Hillhouse, J. W., ed., Deep structure and past kinematics of accreted terranes: American Geophysical Union Geophysical Monograph 50, p. 101–111.

van der Heyden, P., 1992, A Middle Jurassic to early Tertiary Andean-Sierran arc model for the Coast Belt of British Columbia: Tectonics, v. 11, p. 82–97.

Van Fossen, M. C., and Kent, D. V., 1992, Paleomagnetism of 122 Ma plutons in New England and the mid-Cretaceous paleomagnetic field in North America: True polar wander or large-scale differential mantle motion: Journal of Geophysical Research, v. 97, p. 19,651–19,661.

Walker, N., and Brown, E. H., 1991, Is the southeast coast plutonic complex the consequence of accretion of the Insular superterrane? Evidence from U-Pb zircon geochronometry in the northern Washington Cascades: Geology, v. 19, p. 714–717.

Wynne, P. J., Irving, E., Maxon, J., and Kleispehn, K. L., 1995, Paleomagnetism of the Upper Cretaceous strata of Mount Tatlow: Evidence for 3000 km of northward displacement of the eastern Coast Belt, British Columbia: Journal of Geophysical Research, v. 100, p. 6073–6092.

Yeats, R. S., 1977, Structure, stratigraphy, plutonism and volcanism of the Central Cascades, Washington, Part I, General geologic setting of the Skykomish Valley, in Brown, E. H., and Ellis, R. C., eds., Geological excursions in the Pacific Northwest: Bellingham, Western Washington University, p. 265–275.

Zen, E-an, 1988, Tectonic significance of high–pressure plutonic rocks in the western Cordillera of North America, in Ernst, W. G., ed., Metamorphism and crustal evolution of the western United States: Englewood Cliffs, New Jersey, Prentice-Hall, Rubey Volume VII, p. 41–68.